universität wien

MASTERARBEIT / MASTER'S THESIS

Titel der Masterarbeit / Title of the Master's Thesis

„Lipid biomarker signatures in alpine peat bogs in Austria“

verfasst von / submitted by

Katharina Fischer BA

angestrebter akademischer Grad / in partial fulfilment of the requirements for the degree of

Master of Science (MSc)

Wien, 2023 / Vienna 2023

Studienkennzahl lt. Studienblatt / degree programme code as it appears on the student record sheet:	UA 066 855
Studienrichtung lt. Studienblatt / degree programme as it appears on the student record sheet:	Masterstudium Geographie
Betreut von / Supervisor:	Univ.-Prof. Dipl.-Geogr. Dr. Stephan Glatzel
Mitbetreut von / Co-Supervisor:	

Table of contents

Table of figures

List of tables and equations

Abbreviations

ACL	Average Chain Length
BHP	Bacteriohopanepolyol
C	carbon
CH_4	sum formula for methane
cm	centimetre
C/N	carbon to nitrogen ratio
CPI	Carbon Preference Index
C_x	carbon; x = number of carbon atoms
°C	degree Celsius
e.g.	for example
N	nitrogen
n-	“normal” = unbranched
n-C_x	number of carbon atoms in a normal alkane/alkanol
P_{aq}	c
pH	“potential of hydrogen”
PI	Pichlmeier Moor
PM	Pürgschachen Moor
S.	*Sphagnum* moss
µg/g	microgram per gram
WTD	water table depth

Abstract

Anthropogenic actions such as drainages and global warming jeopardize the carbon storage function of peatlands that comprises up to 30% of the global soil organic carbon stock. To save this function, peatlands are mainly rewetted. But microorganisms and typical peat vegetation play also a crucial role in formation of peat and therefore in the sequestration of carbon. Some typical peat plants are expected to be more resistant to microbial degradation. This is indicated by the relative accumulation of recalcitrant chemical compounds such as aliphatic hydrocarbons with further degree of decomposition. In this study, parts of these fraction have been analysed with lipid biomarker analysis for plant-specific markers, degree of decomposition and microbial activity. Study sites are two alpine peat bogs in the Enns valley. Pürgschachen Moor is considered nature-like, Pichlmeier Moor is partly restored. Both emerged after the retreat of a glacier and share the same climate but differ in alteration history. Thus, lipid biomarker analysis aimed to detect signatures of secondary decomposition. But the results of both peat cores show no signs of secondary decomposition. Generally, both peat bogs show similar biomarker distribution patterns. The relative abundance of *Sphagnum* mosses increases with depth, while the contribution of vascular plants diminishes. In both bogs, degree of decomposition is highest in 80cm, which is also supported by the high abundance of microbial biomarkers. Further, microbial biomarkers in the uppermost layer indicate the presence of methanotrophic bacteria living in symbiosis with *Sphagnum*. These results show dynamic processes especially between *Sphagnum* and microorganisms.

Zusammenfassung

Die Kohlenstoffspeicherfunktion von Mooren, die bis zu 30% des globalen Gesamtkohlenstoffs umfasst, ist durch Veränderungen im Wasserspiegel durch den anthropogenen Klimawandel oder Abtorfungen und Drainagen gefährdet. Um dem entgegenzuwirken, werden Moore wiedervernässt. Zusätzlich zum Wasserspiegel spielen typische Torfvegetation und Mikroorganismen eine Rolle an der Bildung von Torf und somit an der Sequestrierung von Kohlenstoff. Einige typische Moorpflanzen sollen robuster gegen mikrobiellen Abbau sein. Ein Indikator dafür ist die Anreicherung von widerstandsfähigen Komponenten wie beispielweise den aliphatischen Kohlenwasserstoffen mit zunehmendem Zersetzungsgrad. Mittels Lipidbiomarker-Analyse wurden Teile dieser Fraktion auf pflanzenspezifische Marker, Dekompositionsgrad und mikrobielle Aktivität untersucht. Untersuchungsgegenstand sind zwei alpine Hochmoore im Ennstal, das naturnahe Pürgschachen Moor und das teilweise renaturierte Pichlmeier Moor. Sie sind beide durch den Rückzug eines Gletschers entstanden und den selben klimatischen Bedingungen ausgesetzt. Da sie sich allerdings in ihrer Nutzungsgeschichte unterscheiden, werden mittels Lipidbiomarker-Analyse auf potentielle Zeichen von sekundärer Dekomposition untersucht. Die Ergebnisse der beiden Torfkerne zeigen keine Anzeichen von sekundärer Dekomposition. Generell zeigen beide Moore gleiche Lipidbiomarker-Verteilungsmuster. Der relative Anteil von Torfmoosen steigt mit der Tiefe, während Marker höherer Landpflanzen schwinden. Die Anwendung von Indizes zeigt die stärkste Dekomposition in der tiefsten Schicht in 80cm Tiefe in beiden Mooren, was durch die Präsenz mikrobieller Biomarker unterstützt wird. Marker für Mikroorganismen weisen in der obersten Schicht auf methanotrophe Bakterien hin, die mit *Sphagnum* in Symbiose leben. Die Ergebnisse zeigen dynamische Prozesse vor allem zwischen *Sphagnum* und Mikroorganismen.

1. Introduction

Peatlands are semi-terrestrial or semi-aquatic ecosystems with a permanently high water table and high accumulation of partially decomposed biomass that was produced sedentarily (Lindsay et al., 2018).

Especially facing anthropogenic global warming, in the past years, peatlands gained scientific but also public interest due to their role in biodiversity, water retention and storage, and their nitrogen and carbon sink function (Rotherham, 2020). Of global impact is particularly the carbon storage function. Although peatlands only cover about 3% of the global land, they are estimated to store between 21 to 30% of the global total soil organic carbon stock (Yu et al., 2010; Leifeld & Menichetti, 2018).

During plant growth, carbon derived from atmospheric carbon dioxide is fixated in the plant structure. When biomass decomposes in an aerobic environment, the bound organic carbon is remineralized as CO_2 into the atmosphere. But in intact peatlands, organic carbon remains in the system and serves as a sink (Rotherham, 2020).

Peatlands can be categorized in minerotrophic and ombrotrophic. Whereas minerotrophic peatlands, called fens, are nourished from mineral soil groundwater, ombrotrophic peatlands, called bogs, are isolated from groundwater, supplied only by precipitation (Rydin et al., 2013). This ‘study’ will be focusing on bogs.

In intact peat bogs, water supply exceeds evapotranspiration, leading to permanently waterlogged and anaerobic conditions in the lower part, the catotelm. There, decomposition of organic matter is decelerated due to lack of easily available oxygen for decomposers. With slow mineralisation, the bound organic carbon is stored in the dead plant material. In the uppermost part, the acrotelm, oxic and anoxic conditions change with the water table depth. Under oxic conditions, vegetation grows and decomposes in this layer. Decomposition rates differ greatly between the two layers. The decomposition rate within the catotelm is only between 0.1 and 7% of the acrotelm. Thus, close to the lowest water table the alteration of peat is highest (Drollinger et al., 2019; Drollinger et al., 2020).

This means that the decomposition rate is correlated with water table depth. Under dry and warm conditions, the water table is low, and decomposition accelerates due to oxygen availability. Whereas cold and moist conditions mean diminished decomposition as a result of a high water level and low oxygen. In this way, the degree of plant decomposition in peat bogs was often used to reconstruct past hydrological conditions at the interface between acrotelm and catotelm (Drollinger et al., 2020; Drzymulska, 2016).

But the water table is also influenced by other factors apart from the naturally occurring seasonal fluctuations (the hydroperiod) that can distort the hydrological reconstruction (Foti et al., 2012; Borgmark & Schoning, 2006). The anthropogenic climate change influences precipitation patterns and increases the frequency of droughts and heatwaves. Without enough precipitation, ombrotrophic peatlands lose their only water supply and are threatened to dry out (Glatzel et al., 2006; Glatzel, 2021).

Anthropogenic interventions like e.g., drainages, peat extractions, agricultural cultivation, or afforestation as well as heats or droughts decrease the water level that much, that already deposited peat in the catotelm is exposed to further fast aerobic decomposition (Rotherham, 2020; Borgmark & Schoning, 2006). This decaying process of already decomposed peat resulting of water table change is called secondary decomposition (Borgmark & Schoning, 2006). With further aerobic degradation, labile carbon is lost as greenhouse gases to the atmosphere (Drollinger et al., 2020). Instead of storing carbon, drained peatlands are becoming a carbon source (Samaritani et al., 2011).

A common measure to mitigate those greenhouse gas emissions by drained peatlands is to restore their former hydrological status by rewetting and to preserve still intact peatlands (Evans et al., 2021).

Although hydrology conditions are a main contributor to peat decomposition rates, Drollinger et al. (2020) and Drzymulska (2016) concluded that decomposition rate is controlled rather by the interaction between biotic - quality of organic matter (plant species and molecular composition) and quality and quantity of microorganisms (fungi, bacteria, invertebrates) - and abiotic factors (e.g., oxygen availability, pH, or temperature) than by one single factor.

In several studies, the degree of peat decomposition in different layers was detected by the application and combination of decomposition proxies such as C/N ratio, FTIR spectroscopy, $\delta^{13}C$ and $\delta^{15}N$ isotope signatures, bulk density, and further calculation of humification indices (Drollinger et al., 2020; Biester et al., 2014; Wang Xinxin et al., 2016; Broder et al., 2012).

Using FTIR spectroscopy, Drollinger et al. (2020), Beer et al. (2008) and Niemeyer et al. (1992) found that with increasing decomposition and depth, certain chemical compounds such as carboxylics, aliphatics, aromatics, and phenolics are residually accumulating in the peat. Those compounds are more recalcitrant to microbial decomposition, especially under energy-deprived conditions within the catotelm. Simultaneously, carbohydrates like polysaccharide decrease as they are easier digestible by microorganisms (Beer et al., 2008; Niemeyer et al., 1992).

Although proxies like FTIR investigate the degree of decomposition, they neither deliver information about plant species present in the peat layers nor about decomposer microorganisms. With increasing depth and decomposition, vegetation composition can at best be determined by the still visible remnants of dominant plants (Drollinger et al., 2020).

1. Research questions

As described above, knowledge about the effects of secondary decomposition on peat and peat parent vegetation in an altered bog can be used to assess the conditions of other peat bogs.

Using lipid biomarker analysis, this study will examine the aliphatic hydrocarbon content of peat in two Alpine peat bogs sharing the same genesis and climate but differing in land use history to investigate the effects of secondary decomposition on the degradation processes. They serve as both indicators for peat composition but can also determine the degree of decomposition (Schellekens et al., 2015). Considering this, the research questions will be:

- Is there a detectable difference in the peat decomposition along a degradation gradient pattern due to secondary decomposition comparing Pürgschachen Moor with Pichlmaier Moor using lipid biomarker analysis?
- Are plant species-specific biomarkers detectable? Can species composition be reconstructed? Is there a species-specific decomposition gradient?
- Can microbial activity be detected by lipid biomarker analysis? Does it occur with higher degrees in decomposition?

Both bogs, Pürgschachen Moor and Pichlmeier Moor have already been subject to research, also about decomposition and secondary decomposition. By FTIR spectroscopy and other decomposition proxies, Drollinger et al. (2020) found that both bogs showed signs of secondary decomposition due to anthropogenic or climatic water table changes. Although, decomposition in Pichlmeier Moor was much more pronounced than in Pürgschachen Moor.

1.1. Background

Lipids such as aliphatics, phenolics and carboxylic acids are already established biomarkers for the detection of peat composition, decomposition, and microbial contributions (Lehtonen & Ketola, 1993; Naafs et al., 2019). Research on aliphatic hydrocarbons has first been applied in petrology but has abundantly been conducted in organism like bacteria and plants for a long time (Killops and Frewin, 1985).

Aliphatic hydrocarbons are specifically suited for investigations of organic matter because they are a main constituent of cellular membranes of eucaryotes, prokaryotes and archaea where they often rigidify the cell wall (Peters et al., 2004).

The presence of specific compound classes (like *n*-alkanes, *n*-alkanols, or terpenoids) and single molecules of aliphatic hydrocarbons often provide information about the source organism. Structural characteristics like the position of a functional group or side chain on the hydrocarbon skeleton or unsaturation gives insight into processes or chemical conditions within the systems.

In the following sections, aliphatic compound classes commonly identified in peatlands will shortly be introduced (e.g., Bhattacharya et al., 2021; Serebrennikova et al., 2018; Ortiz et al., 2011).

1.1.1. *n*-alkanes

n-alkanes are saturated hydrocarbons. They consist of chains of C_nH_{2n+2} with n= 1, 2, …, x and build series of homologues (Fig. 1). CH_4 is the simplest *n*-alkane. The prefix 'n' indicates 'normal' meaning unbranched (Mortimer and Müller, 2010).

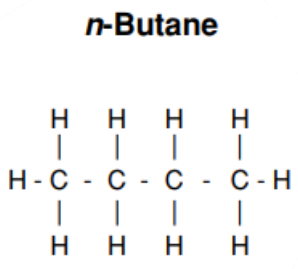

Figure 1 The homologue n-butane with C_4H_{10} as example for unbranched alkanes (Peters et al., 2004)

Long hydrocarbon chains with 27 to 35 carbon atoms are mainly produced by higher plants, mid length hydrocarbon chains of 23 to 25 carbons by mosses and aquatic macrophytes. A few microorganisms can also synthesize long-chain *n*-alkanes, but they predominantly synthesize short chain homologues with C_{15} to C_{21} (Bhattacharya et al., 2021; Peters et al., 2004).

Due to their shortage of functional groups and their insolubility in water they are relatively resistant to microbial degradation (Lehtonen & Ketola, 1993; Naafs et al., 2019; Peters et al., 2004).

1.1.2. *n*-alkanols

n-alkanols are produced through reduction of *n*-C_{16} fatty acids and form homologues of $C_nH_{2n+1}OH$ (Fig. 2).

Figure 2 The homologue nonadecan-1-ol $C_{19}H_{40}O$. Each tooth indicates a CH_2 group, the left end is substituted with a methylene group ($-CH_3$) (NIST Chemistry WebBook)

Like *n*-alkanes, different homologues of *n*-alkanols are produced by different organisms, although distribution between source species overlap greatly. Short-chain *n*-alkanols between C_{12} and C_{26} are dominant in algae and bacteria, mid-chain *n*-alkanols between C_{22} and C_{24} are abundant in submerged plant species, and long chain homologues from C_{22} to C_{28} are formed by vascular plants or lichens. *n*-alkanols of plants typically have a strong even*n*-over-odd predominance in contrast to *n*-alkanes (Zhou et al., 2010; Naafs et al., 2019).

1.1.3. Triterpenes

Triterpenes are structurally diverse lipids that consist of six isoprene units. Their parent molecule is the acyclic squalene (Fig. 3). In bacteria, plants and animals that are expected in a peatland environment, especially tetracyclic and pentacyclic triterpenes are abundant (Naafs, et al., 2019; Pancost et al., 2002; Pancost et al., 2003).

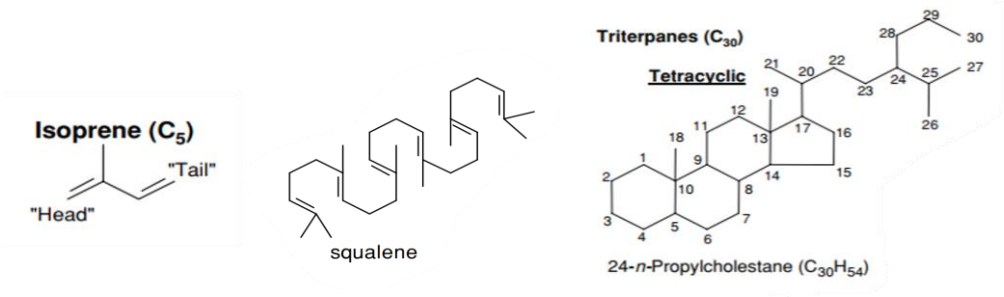

Figure 3 Isoprene (left) as the precursor molecule of squalane (middle). In the biosynthetic pathway, triterpenoids (right) derive from squalene (Peters et al., 2004; Mortimer and Müller, 2010).

Eukaryotes predominantly synthesize tetracyclic triterpenes called steroids. Pentacyclic triterpenoids can be produced by plants and bacteria but can be easily distinguished due to their structural characteristics (Naafs et al., 2019).

1.1.3.1. Tetracyclic triterpenes - Sterols

Sterols are tetracyclic triterpenes that are commonly synthesized in eukaryotes. In plants, they are often contained in hormones, or membrane compartments, or in the epicuticular leaf waxes of higher plants.

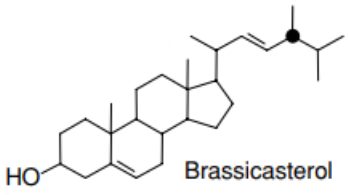

Figure 4 Chemical structure of the C_{28}-steroid brassicasterol. This molecule is especially abundant in plants (Peters et al., 2004).

The most abundant sterols in plants named phytosterols are built of 27 to 30 carbon atoms, where the most abundant is C_{29} (Fig. 4). Despite the presence of steroids in peat-forming plants, species specific sterol signatures were not discovered yet, because phytosterols are abundant

in every plant. Sterol composition varies greatly even within in single plant parts (Naafs et al., 2019; Wöstmann, 2007).

1.1.3.2. Pentacyclic triterpenes

Pentacyclic triterpenoids are structurally characterized by five rings. In peat, they derive mainly from vascular plants and bacterial input (hopanoids) (Naafs et al., 2019).

1.1.3.3. Plant derived pentacyclic triterpenes

Similar to steroids, pentacyclic triterpenoids serve as cell wall rigidifiers but are mainly present in epicuticular plant leaf waxes of vascular plants (Fig. 5) (Lehtonen and Ketola, 1993; Philp, 1985).

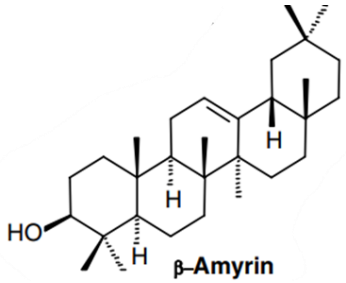

Figure 5 The pentacyclic ß-amyrin is found in many angiosperms such as the dandelion (Peters et al., 2004).

Their abundance and variety have no species-specific trend. Therefore, they serve as indicator of the presence of higher terrestrial plants in general (Wöstmann, 2007).

1.1.3.4. Bacterial pentacyclic triterpenes - Hopanoids

Hopanoids are pentacyclic triterpenes produced exclusively by bacteria. As they predominantly appear in the upper peat layers, they are expected to be produced by aerobic bacteria, among them methanotrophs (Op den Camp et al., 2010; Naafs et al., 2019). Therefore, they indicate microbial activity and oxic conditions.

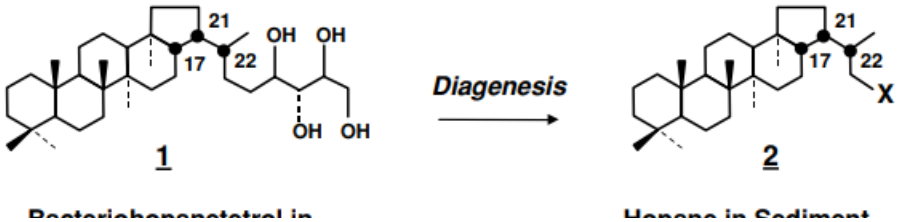

Figure 6 Production of hopane (right) by diagenetic alterations of the bacterially produced bacteriohopanetetrol (Peters et al., 2004)

Hopanoids can be divided into simple hopanoids with a ring system consisting of 30 carbon atoms, and more complex ones called bacteriohopanepolyols (BHP) (Inglis et al., 2018). After production, BHP is diagenetically degraded, meaning chemical and physical alterations of buried organic or inorganic matter, and results in hopane (Fig. 6) (Peters et al., 2004). Many studies focus only on hopanes, as for BHPs additional laboratory analysis is necessary.

2. Methods

2.1. Study sites

The Pürgschachen Moor and the Pichlmeier Moor are two peat bogs that lie in the inner Enns valley in Austria on about 632m a.s.l. (Drollinger et al., 2019). Surrounded by the mountains of the Gesäuse, they are the remnants of a series of valley floor bogs. They started to grow almost 10,000 years ago in the basin of a postglacial lake on impermeable clay after the retreat of the Enns glacier (Moorschutzverein Pürgschachen; Amt der steiermärkischen Landesregierung). Located in the same valley, they also share the same climate with a mean air temperature of 7,27+-0,71°C and an average annual precipitation of 1248+-158mm (1987-2016) (Drollinger et al., 2020). Peat accumulation rate in both mires is on average 0,69 mm per year (Drollinger et al., 2019; Amt der steiermärkischen Landesregierung).

Pürgschachen Moor is the only of the valley mires that is considered as an intact peat bog. All the others have been degraded by peat cutting, agriculture, or forestation (Amt der steiermärkischen Landesregierung). Human intervention on the peatlands started in 1908, when the Enns River was regulated resulting in a lowering in the water level. This was continued by agricultural cultivation, drainage, and peat extraction (Winterer, 2019).

In Pürgschachen Moor, peat extraction was only conducted for a short time in a small area on the southern edge of the bog. Pürgschachen Moor is under conversation since 1976, protected by Ramsar since 1991, and declared as a bird reserve and FFH- habitat since 2006 (BMLRT, 2022; Amt der steiermärkischen Landesregierung).

The bog has an extent of 62ha, is covered by natural pine bog vegetation and considered the "biggest largely intact valley peat bog in Austria with a closed peat moss cover" (Drollinger et al., 2019). The peat thickness is expected to be 7-8m. The average water table depth is about 12cm in the centre and about 21cm on the edge area. Minimum water level is 29cm in the centre and 28cm on the edge (table 1) (ibidem).

Pichlmeier Moor lies about 5km to the east of Pürgschachen Moor. Its peat thickness is about 2-3m. This bog was influenced by extensive alteration with peat cutting, afforestation, and cultivation and shows varying drainage depths and ditches (Winterer, 2019). The maintenance of the drainage system stopped in the 1990s, but it is still draining the east side of the bog. The western section of the bog including former drainage pools is considered as the modern peat cutting site and currently flooded and overgrown by natural vegetation succession (Drollinger et al., 2020). Due to its heterogeneity, Pichlmeier Moor is categorized in various biotope types with differing conditions. According to the "Fachbericht Moore", eight FFH-biotope types are found on the bog. The area where the sample for this study originates, is considered as still capable of renaturation. (Moorschutzverein Pürgschachen, 2005).

Water table depth varies greatly all over the peat bog. Unfortunately, there is no data available for the exact spot where the samples were taken. But in Drollinger et al. (2019) and Moorschutzverein Pürgschachen (2005), the water table depth was measured in the younger formerly peat cutting site close by (table 1)

Table 1 Water table depth in PM and PI according to Drollinger et al., (2019) and Moorschutzverein Pürgschachen (2005)

	Water table depth [cm] below surface			
Location	Minimum	Maximum	Average	Median
PM	28 - 28,5	4	11,8	-
PI	43 - 56,5	24,5 - 28,5	-	29 - 32,5

The average water table depth at the younger formerly peat cutting site is 40cm with a minimum of 53cm and on the older peat cutting sites the average is around 35 the minimum around 53cm (Drollinger et al., 2019). Figure 7 shows the sampling locations.

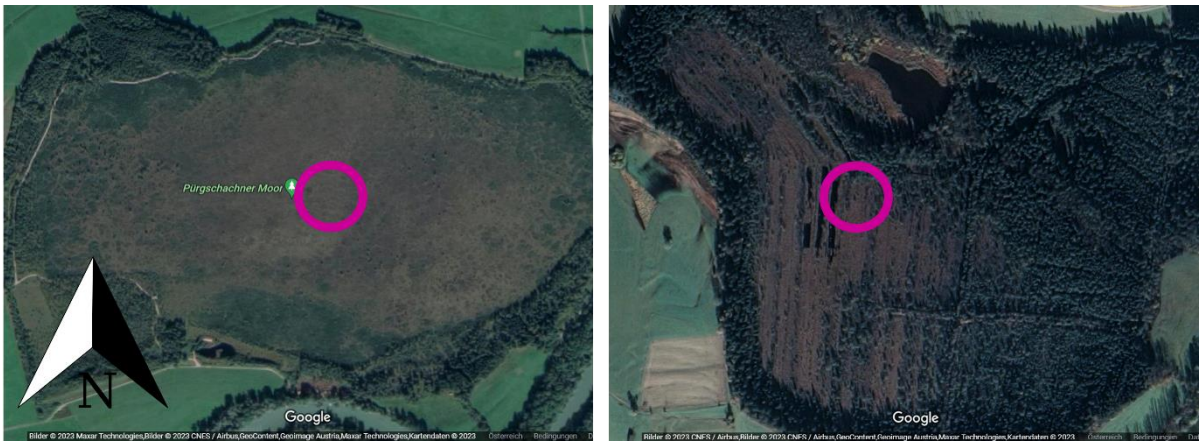

Figure 7 Sampling locations encircled in pink in Pürgschachen Moor (left) and Pichlmeier Moor (right) (Maps Data: Google, ©2023 Maxar Technologies, ©2023 CNES/Airbus, GeoContent, Geoimage Austria, Maxar Technologies)

2.2. Sampling

In total, two peat cores were taken with a Russian peat corer. One core originates from the very centre of the Pürgschachen Moor (PM1) which is treeless and inhabited by natural peat bog vegetation such as *Sphagnum sp., Eriophorum vaginatum, Rhynchospora alba, Pinus mugo,* but also *Calluna vulgaris*. The second core was taken in the north-western part of Pichlmeier Moor, a former peat cutting site with natural succession with *Calluna vulgaris, Vaccinium vitis-idaea, Betula pubescens, Pinus sylvestris,* and *Sphagnum sp.* (Drollinger et al., 2019). As mentioned above, the core originates from thick peat in a revitalization stage.

The cores were cut into sections at the depths of 10cm – representing the acrotelm, 30cm – representing the interface between acrotelm and catotelm that is influenced by a fluctuating water table, and 80cm – representing the permanently waterlogged catotelm, for PM and PI. As the extracted cores are thin and peat contains large amounts of water, several cores needed to be taken.

Further, fresh biomass of the main peat-constituting plant *Sphagnum* ssp. and of *Calluna vulgaris* and *Pinus mugo* representing the dominant vascular plants was sampled at Pürgschachen Moor to compare the lipid distribution pattern of fresh with decayed material.

2.3. Laboratory

In the laboratory, the samples were frozen, freeze-dried, grinded, and homogenized (Fig. 8). Subsequently, they were analytically prepared for measuring in the GC-FID and further GC/MS.

Figure 8 Freeze-dried peat samples (left) and in jars (right) Calluna vulgaris, Pinus mugo and Sphagnum ssp.

2.3.1. Lipid extraction

The samples needed to weigh approximately 2g freeze-dried. For later interpretation of the results, following standards were added (100µl each): squalane (99 µg/ml) for the hydrocarbons and 1-nonadecanol (101 µg/ml) for the alcohols. To extract the volatile and bound fatty acids, the samples were saponified with 50ml of potassium hydroxide (6% in methanol) for two hours at 70°C in the oven and centrifuged several times and then decanted into a separation funnel afterwards. To extract as much organic molecules as possible, the remaining sediment was diluted with a 3:1 mixture of dichloromethane and methanol, put in an ultrasonic bath for 15 minutes, centrifuged, and the resulting solution was poured into the separation funnel. This process was repeated until the solution became clear. To fully extract the organic matter, the pH value had to be changed. Therefore, pure water and hydrogen chloride were added, the separation funnel was shaken very carefully. After at least one hour, two phases become clearly distinguishable. The lower phase is the organic matter within the solvents (Fig. 9).

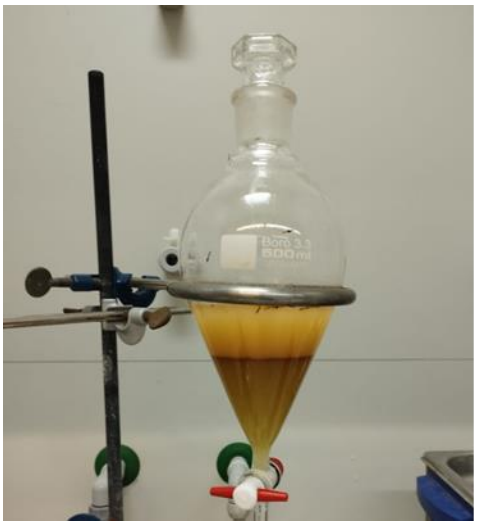

Figure 9 Extraction of organic matter of a peat sample. The upper phase contains inorganic or unsoluble compounds. The upper one the extractable organic matter.

To ensure that no water is bound to the organic molecules, the organic fraction was cleaned by running through a filter with glass wool and $NaSO_4$. Afterwards, the solvents were vaporized in a rotary evaporator, so that only the extracted organic molecules remained. As the samples still contained asphaltenes which would damage the GC, they were diluted with hexane and filtered again through a glass wool and $NaSO_4$ filter several times. In this step, the maltenes were separated from the asphaltenes.

The maltenes were further separated into the final fractions of hydrocarbons, ketones, alcohols, and carboxyl acids by liquid chromatography. Although the result of the extraction of organic compounds were four fractions, in this thesis, only two of them – the hydrocarbon and the alcohol fraction – were used for further interpretation.

The maltene-fraction as mobile phase was applied on an aminopropyl column as stationary phase (Fig. 10). The fractions were eluted with hexane for the alkanes and with dichloromethane and acetone (9:1) for the alcohol fraction.

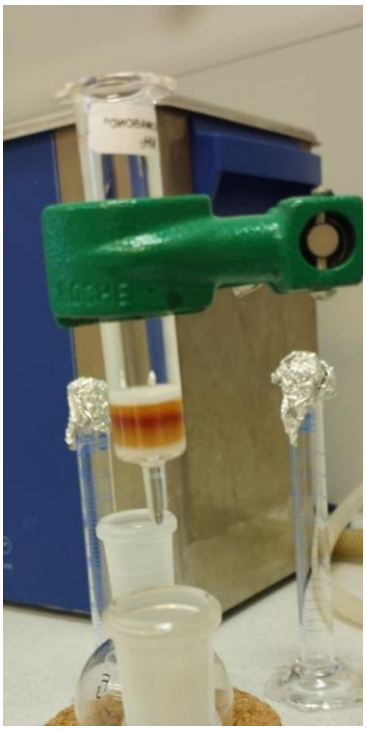

Figure 10 Extracted organic matter (coloured part in the column) in the aminopropyl column

Due to the polarity and low volatility of alcohols, they need to be derivatised with N,O-bis(trimethylsilyl)trifluoroacetamide. The hydrogen atom in the OH-group of the alcohol is being replaced by a trimethylsilyl group. After putting the sample in the oven for one hour at 70°C it ready to be measured in the GC-FID and GC/MS (Fig. 11).

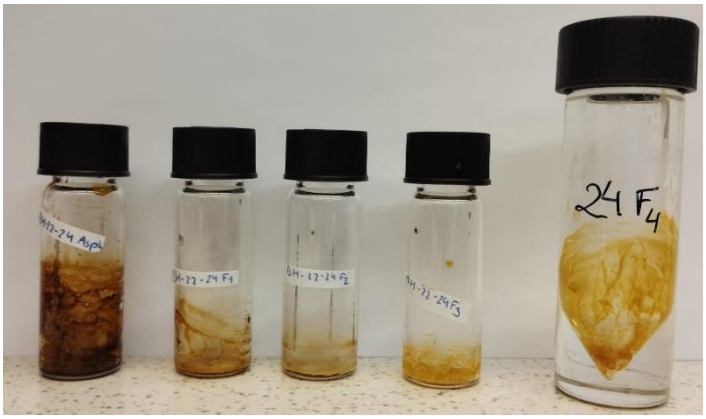

Figure 11 Results of lipid extraction from left to right: asphaltenes, hydrocarbons, ketones, alcohols and fatty acids.

2.3.2. Analysis in GC-FID and GC/MS

For being measured in a gas chromatograph (GC), the analytes need to be volatile. Therefore, it is first led through a column, where the volatile components are being evaporated. This gaseous phase is then led through an inert carrier gas – the stationary phase. There, the compounds are being separated by their molecular mass. After passing the column, the carbon containing components come into a flame-ionization chamber, where they are oxidized and ionized to cations, and then accelerated to a negatively charged collector plate. The measured electric current is coupled with the carbon atoms that are oxidized in the flame (Sparkman et al., 2011; McMaster et al., 2008; measurelabs: GC-FID).

GC-FID detects the relative abundance of all molecules in the extract of a sample which is depicted by peaks in a chromatogram. The heavier a molecule, the longer it takes to reach the detector. While the GC-FID is used for quantification of the molecules inside a sample, it doesn't provide information about the quality of the organic matter.

Identification of the molecules that lie behind each peak of the chromatogram is done by measuring the same sample in the GC/MS.

In a GC/MS, the sample first runs through a gas chromatograph and is being separated in a column with an inert carrier gas just like in the GC above mentioned. Instead of a FID, the molecules are led to a mass spectrometer after passing the GC (Schwedt, 1996; McMaster et al., 2008).

A mass spectrometer detects the molecular weight and structure of unknown particles. It measures the mass-to-charge ratio of charged fragments, that have been ionised before in the MS (Sparkman et al., 2011). This provides three-dimensional data including a chromatogram and mass spectra, combining the results of GC and MS (McMaster et al., 2008). More precisely, it reveals how many ions of a certain mass-to-charge ratio (m/z) were detected after what time. By interpreting these io*n*-peaks, the types and structures of the molecular components can be determined.

Samples were measured at the laboratory of the Institute of Geology in Hamburg with a GC-FID Thermo Scientific Trace GC 1310 with flame ionisation detector for quantification and a GC-MS Thermo Scientific Trace GC Ultra coupled to a Thermo Scientific DSQII mass spectrometer.

2.4. Identification of molecules

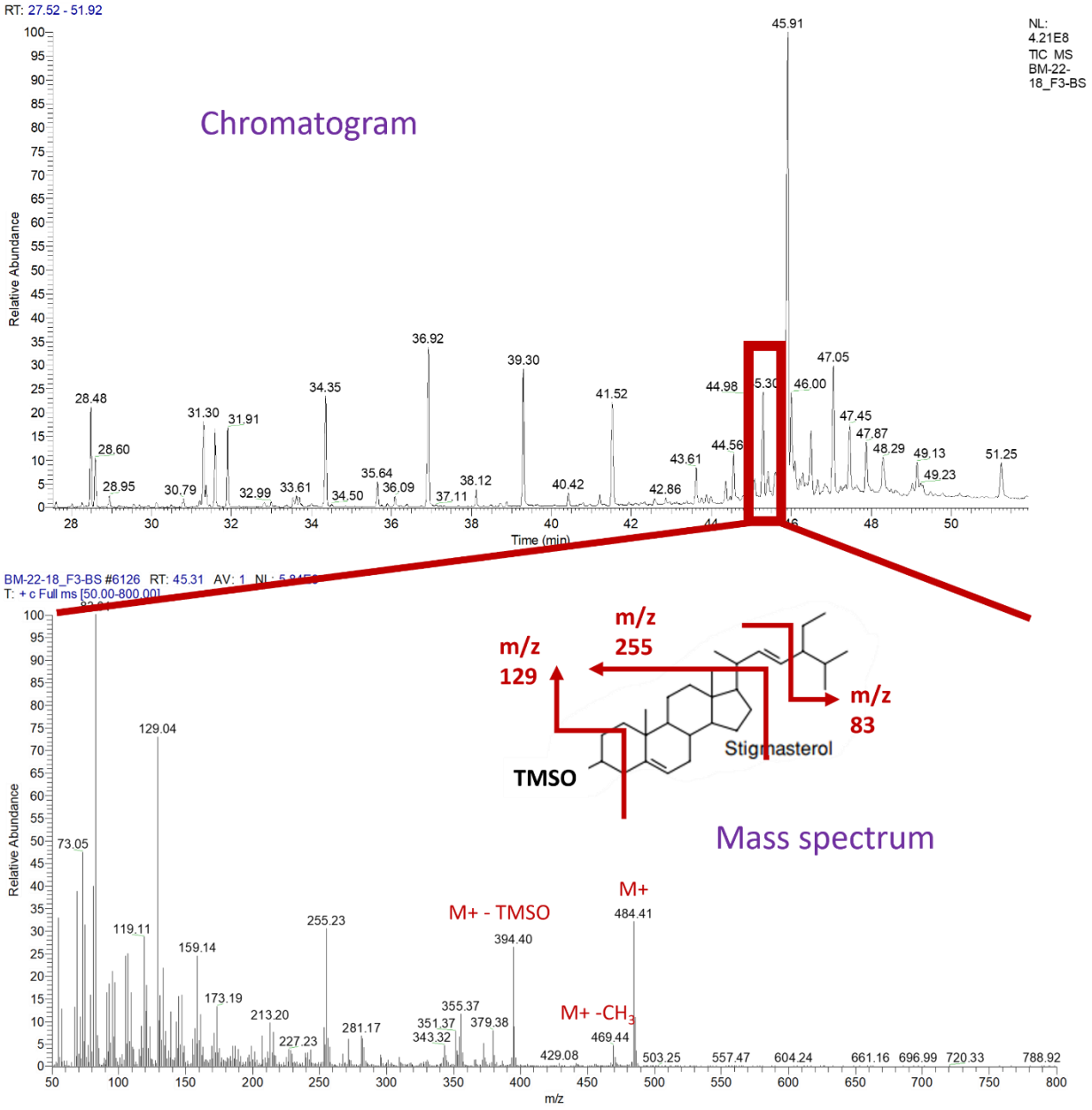

Figure 12 Example of component identification. The chromatogram above shows all molecules of a sample represented each by a peak. Behind each peak lies a mass spectrum (below) that shows the fragmentation pattern of the molecule(s). In this picture, the typical fragmentation pattern of stigmasterol-TMSO (derivatized) is shown. (Source: Screenshot from own analysis (Xcalibur DAIS), chemical structure of stigmasterol: Peters et al., 2004)

To identify molecules through the mass spectrum, the molecular ion peak or parent peak (M^+) with the highest m/z needs to be determined (Fig. 12). M^+ represents the molecular weight of the whole molecule. During fragmentation in the MS, each molecule breaks in characteristic

ways, enabling a differentiation between isomers (Peters et al., 2005). The most abundant fragment ion is called base peak. Some groups of chemical components fragment in the same way and can also be identified by the base peak.

N-alkane homologues for example break along their CH_2-groups, producing a characteristic fragmentation pattern by differing only by 14amu and exponential decrease in abundance with increasing mass. *N*-alkanes usually have their base peaks at m/z 71, m/z 57, or m/z 99 (Philp, 1985). Hopanoids can be identified by the base peak at m/z 191 (Bhattacharya et al., 2021; Philp, 1985). All other components are identified with help of literature and of the library NIST Chemistry WebBook. Identification of the alcoholic compounds were difficult. Through derivatisation, the components gained extra m/z 73 and fragmentation patterns changed. NIST entries of those compounds were very scarce.

For interpreting mass spectra, Xcalibur Data Acquisition and Interpretation Software by Thermo Fisher was used. For quantification OpenChrom by Lablicate.

2.5. Calculation of indices

Several values and indices based on *n*-alkanes can give insight into peat composition. Whether source of organic matter derives mainly from microorganisms, mosses, or higher terrestrial plants can be determined with CPI. The ACL detects changes in species composition and distinguishes between plants thriving in either drier or wetter conditions. P_{aq} and the *n*-C_{23}/*n*-C_{29} and *n*-C_{25}/*n*-C_{29} ratios reflect the input of aquatic/submerged versus vascular plants. (Bhattacharya et al., 2021).

All these indices are based on the specific *n*-alkane distribution pattern of certain species as described above.

It is important to mention that these indices are only relative measures and that none of them is standardized. Variables and even formula vary greatly between studies depending on e.g., ecosystem, dominant vegetation, climate (Ficken et al., 1998; Andersson et al., 2012; Serebrennikova). Therefore, interpretation of the indices should be handled with care and only used together with other markers (Andersson et al., 2012; Naafs et al., 2019).

2.5.1. Carbon Preference Index

The Carbo*n*-Preference-Index (CPI) measures odd-over-even predominance of *n*-alkanes. As described above, indicate odd carbon chains input of fresh organic matter, whereas even *n*-alkanes are degradation products.

Therefore, it applied for assessing the degree of post depositional alteration in organic matter. CPI values are higher when the contribution of plants is high hence organic matter is well preserved. In contrast, a lower CPI indicates either high abundance of microorganisms or higher degradation (He et al., 2019; Bhattacharya et al., 2021).

In this study, CPI was calculated according to Ficken et al. (1998) (formula 1) as they investigate also in the lipid signature of ombrotrophic peat bogs with similar vegetation.

$$CPI_{n-alkane} = \frac{2\times(C_{23}+C_{25}+C_{27}+C_{29}+C_{31})}{(C_{22}+C_{24}+C_{26}+C_{28}+C_{30})+(C_{24}+C_{26}+C_{28}+C_{30}+C_{32})} \quad (1)$$

$$(Ficken\ et\ al., 1998)$$

According to Naafs et al. (2019), fresh biomass has a CPI from 4-40. It varies greatly depending on species composition. CPI values of peats dominated by *Sphagnum* range from 10-35, while those dominated by woody species or graminoids lie between 5 and 15. Values below are attributed to microbial degradation and diagenetic effects (Naafs et al., 2019; Andersson et al., 2012).

2.5.2. ACL

The Average Chain Length of *n*-alkanes (ACL) can determine the source of the organic matter by calculating the most abundant chain-length of mid- to long-chain *n*-alkanes (Li et al., 2018).

The ACL is used for reconstruction of climatic changes (Naafs et al., 2019). The distribution of *n*-alkanes would reflect the response of vegetation to changing climatic conditions. In drier climate, predominantly vascular plants from *n*-C_{27} to *n*-C_{35} would be present. In contrast, in colder and more humid climates, submerged plants like mosses with distributions of *n*-C_{23} to *n*-C_{25} would thrive. Nevertheless, the ACL cannot provide information about which climatic

changes occurred. As with the CPI, the *n*-alkane homologues added to this equation are selected by the expected dominant species.

Although ACL was also adapted to typical ombrotrophic peat bog vegetation, it did neither include *n*-C_{23} nor *n*-C_{25} (Wöstmann, 2007). The two peat bogs examined in this thesis are *Sphagnum* dominated bogs. Therefore, here, ACL is calculated as in Ficken et al. (1998) (2).

$$ACL = \frac{23\times C_{23}+25\times C_{25}+27\times C_{27}+29\times C_{29}+31\times C_{31}+33\times C_{33}}{C_{23}+C_{25}+C_{27}+C_{29}+C_{31}+C_{33}} \quad (2)$$

$$(Ficken\ et\ al., 1998)$$

2.5.3. Paq and others

Similar to the ACL, the P_{aq} investigates in plant species distribution but is specifically designed for aquatic environments (Ficken et al., 2000). As peatlands are semiaquatic ecosystems and many submerged plants also occur there, it has been widely applied to wetlands. The higher the P_{aq} value, the wetter conditions are expected to be (Bhattacharya et al., 2021).

$$P_{aq} = \frac{(C_{23}+C_{25})}{(C_{23}+C_{25}+C_{29}+C_{31})} \quad (3)$$

$$Ficken\ et\ al., (2000)$$

Although higher plants can synthesize long chain *n*-alkanes up to *n*-C_{35}, they often have their maxima at *n*-C_{27}, *n*-C_{29} and *n*-C_{31} and barely synthesize *n*-C_{23} and *n*-C_{25}. Whereas in most *Sphagnum* species, the *n*-alkanes C_{23} and C_{25} dominate (Zhang et al., 2016).

Nevertheless, some *Sphagnum* species exhibit maxima *n*-C_{31} but most of them lack the *n*-C_{29} (Bingham et al., 2010; Baas et al., 2000; Pancost et al., 2002). Therefore, for a direct comparison of *Sphagnum* species vs. higher terrestrial plants, P_{aq} can be supplemented by the ratio of *n*-C_{23}/*n*-C_{29} and *n*-C_{25}/*n*-C_{29}.

Further, *Sphagnum* species that prefer drier and aerated conditions are found to exhibit a peak at *n*-C_{25}, whereas *Sphagnum* species favouring humid and submerged conditions maximize at *n*-C_{23} (Zhang et al., 2016). Calculating the ratio of *n*-C_{23}/*n*-C_{25} can therefore also infer species composition of *Sphagnum* and redox conditions in peat.

3. Results

The results for all identified molecules and calculated indices in this study are described in the following. Molecules are grouped in the chemical compound classes discussed in the introductory section.

As mentioned above, each peatland is represented by three samples at the depths 10cm, 30cm and 80cm. Therefore, the sampling code consists of the abbreviation for the bog (PM for Pürgschachen Moor and PI for Pichlmeier Moor) and the number of the according depth (10, 30, 80). Further, the biomarker distribution of the two plant samples *Calluna vulgaris* and *Sphagnum ssp*. will be discussed. Biomarkers of *Pinus mugo* were also extracted and measured but could not be interpreted due to contamination and/or co-elution.

3.1. Distribution of compound classes

The organic compounds detected in the samples were *n*-alkanes, *n*-alkanols, and the terpenoids steroids, pentacyclic triterpenoids and hopanoids (table 2).

Generally, both peat bogs exhibit similar depth trends in all compound classes except for hopanoids. PM30 and PI30 contain the smallest amount of lipids (79µg/g and 415µg/g), although lipid concentration in PI is five times higher. The highest total lipid concentrations are found in PM80 and PI80 (2142µg/g and 2012µg/g). In both bogs, steroids and hopanoids peak in 80cm depth, while pentacyclic triterpenoids have their minimum in this depth.

n-alkanes exhibit a clear maximum in 30cm depth in PM and PI (11µg/g in PM, 88µg/g in PI). In PM, *n*-alkanols are highest in 10cm depth. In PI, their concentration equals n PI10 and PI30.

Concerning total compound concentrations, steroids are by far the most abundant group in both bogs (2310µg/g in PM and 1862µg/g in PI), followed by *n*-alkanols (1281µg/g in PM and 1049µg/g in PI). *n*-alkanes are the compound classes with lowest concentrations, although they are considerably lower in PM (in total 28µg/g) than in PI (in total 109µg/g).

PM contained more hopanoids than PI. Distributions differ between the peatlands. Whereas in PM, concentration and relative abundance are lowest at 30cm, they gradually increase downcore in PI.

Archaeol was also detected and is further added to the group of hopanoids as it is also a terpenoid synthesized by microorganisms.

Table 2 Abundances of chemical compound classes in µg/g and % in all peat samples and in Calluna and Sphagnum. The column furthest to the rights shows the sum of identified biomarkers per sample in µg/g. The total abundance of each compound class over all peat samples is presented in the last row.

Sample	*n*-alkanes		*n*-alkanols		Steroids		Pentacyclic triterpenoids		Hopanoids + Archaeol		Sum lipids per sample
	µg/g	%	µg/g	%	µg/g	%	µg/g	%	µg/g	%	[µg/g]
PM10	7	0,40%	702	39,60%	947	53,5%	44	2,5%	69	3,60%	**1763**
PM30	11	14,00%	30	37,60%	24	30,4%	12	15,5%	3	1,30%	**79**
PM80	10	0,40%	549	25,40%	1339	61,9%	30	1,4%	214	9,90%	**2142**
Sum per compound in PM [µg/g]	28		1281		2310		86		279		
PI10	10	1,10%	485	54,10%	370	41,3%	26	2,9%	3	0,40%	**894**
PI30	88	20,70%	77	20,86%	126	34,0%	120	32,3%	4	0,90%	**415**
PI80	11	0,50%	487	23,80%	1366	66,7%	16	0,8%	131	6,40%	**2012**
Sum per compound in PI [µg/g]	109		1049		1862		162		138		
Calluna	91	5,00%	922	51,00%	675	37,3%	106	5,9%	2	0%	**1796**
Sphagnum	15	0,30%	1161	19,80%	4617	78,5%	0	0,0%	0	0%	**5793**

The two classes predominantly produced by plants, pentacyclic triterpenoids and steroids, show inverse depth trends. While steroid concentration drastically increases from 30cm to 80 cm, whereas pentacyclic triterpenoid contribution decreases. While the triterpenoids account only for 1,4% and for 0,8% of the peat in 80cm at PM and PI, the contribution of sterols increase to 62% and 67% in 80cm depth at PM and PI.

Calluna vulgaris total lipid concentration with 1796µg/g is similar to PM10. In contrast to the peat samples, exhibits *Calluna* strong maximum in *n*-alkanols (comprising 51% of the identified lipids). *n*-alkane concentrations of 91µg/g are the smallest class besides hopanoids with 2µg/g.

Of all measured samples, *Sphagnum* is richest in identified components with 5793µg/g. Almost 80% of the identified lipids in *Sphagnum* are steroids. There were neither pentacyclic triterpenoids nor hopanoids detected.

3.2. *n*-alkanes

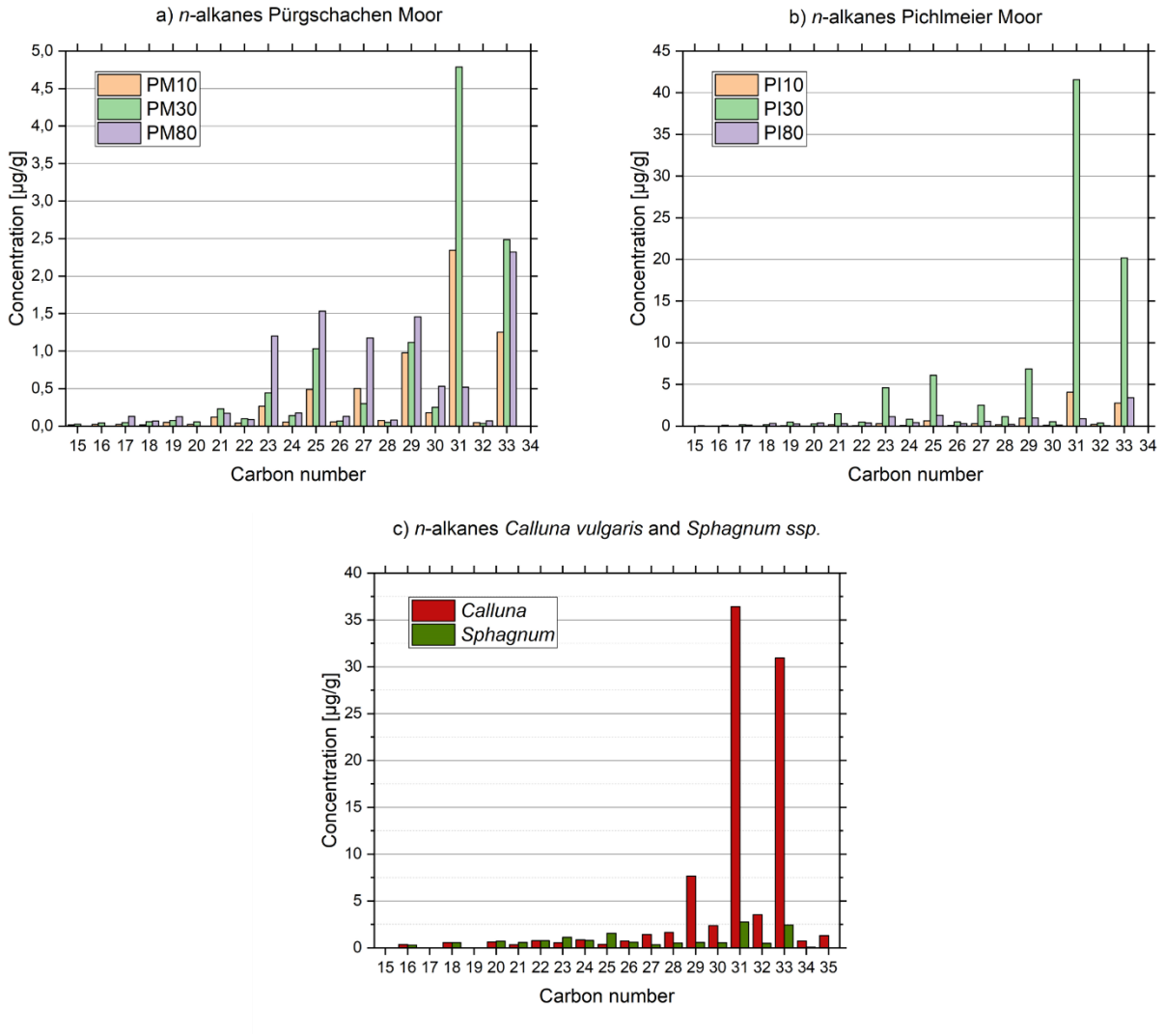

Figure 13 (a) distribution of n-alkanes per carbon chain *number [µg/g dw] in peat samples of Pürgschachen Moor, Pichlmeier Moor, and (c) Calluna vulgaris and Sphagnum* *(b)*

In peat samples, *n*-alkanes ranged from C_{15} to C_{33} with a strong odd over even predominance between C_{21} and C_{33} (Fig. 13a, b, c). Plants contained *n*-alkanes between C_{16} to C_{35}. Almost all samples, including plants, have their highest peak at *n*-C_{31}.

Both peatlands share the same *n*-alkane distribution pattern (Fig. 13a and b). The most abundant *n*-alkanes are odd mid- and long-chain *n*-alkanes from C_{23} to C_{33}. PM10, PI10, PM30 and PI30 have their maxima at *n*-C_{31}, ranging from 2µg/g in PM10 to 42µg/g in PI30. *n*-C_{33} exhibits the second highest peaks with values from 1µg/g in PM10 to 20µg/g PI30. In contrast, two

deepest samples at 80cm show highest abundances at *n*-C_{33} (with 2µg/g in PM80 and 3µg/g in PI80), followed by *n*-C_{29} (1,5µg/g in PM80 and 1µg/g in PI80).

In all peat samples of PM and PI, the mid-chain *n*-alkanes *n*-C_{23} and *n*-C_{25} that are typical for *Sphagnum* mosses have also pronounced peaks up to 5µg/g of *n*-C_{23} and 6µg/g of *n*-C_{25} (PI30). Short chain *n*-alkanes from *n*-C_{15} to *n*-C_{20} are present in relatively low concentrations with maximum 0,5µg/g (*n*-C_{19} in PI30).

The *n*-alkane distribution in *Sphagnum* biomass sample (Fig. 13c) exhibits most abundant peaks at *n*-C_{31} (3µg/g) and *n*-C_{33} (2µg/g), and second maxima at *n*-C_{25} (2µg/g) and *n*-C_{23} (1µg/g).

Calluna vulgaris shows distinctively high concentrations of *n*-C_{31} (36µg/g) and *n*-C_{33} (31µg/g) (Fig. 13c). Only marginal amounts of *n*-C_{23} and *n*-C_{25} were detected, but comparably high values of *n*-C_{29} (7,7µg/g).

3.3. *n*-alkanols

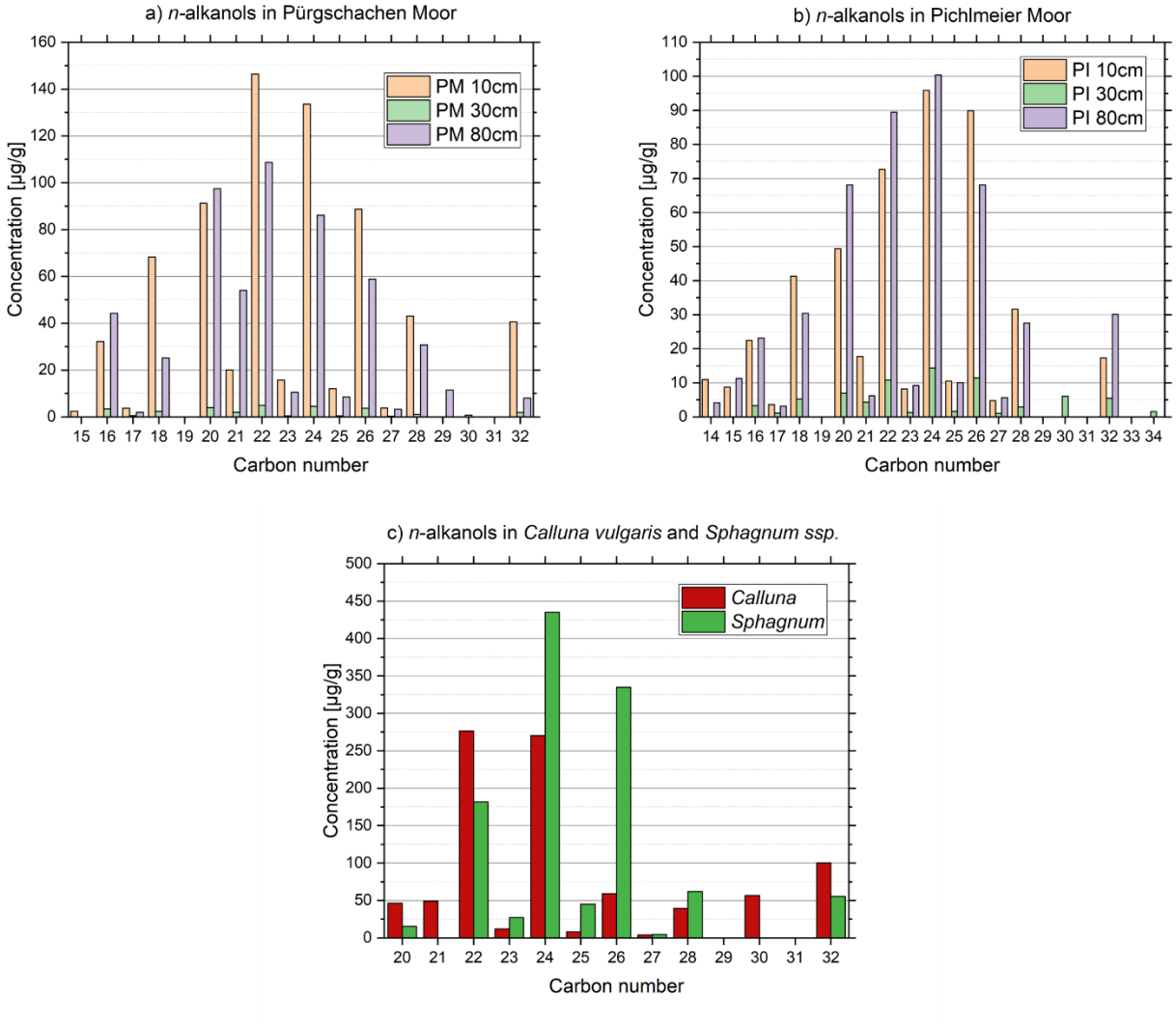

Figure 14 (a) distribution of n-alkanols per carbon chain *number [µg/g dw] in peat samples of Pürgschachen Moor, (b) Pichlmeier Moor, and (c) Calluna vulgaris and Sphagnum*

Overall, *n*-alkanols ranged from *n*-C_{14} to *n*-C_{34} with a strong even over odd predominance (Fig. 14a, b, c). In PI, also *n*-C_{14} was found in PI10 an PI80, and *n*-C_{34} in PI30.

n-alkanol distribution patterns are similar in both bogs. The mid-chain lengths from *n*-C_{20} to *n*-C_{26} are dominant. Nevertheless, all samples in PM have their maximum at *n*-$C_{22,}$ whereas in PI, all samples climax in *n*-C_{24}. The second peak in PM10 and PM30 is at *n*-C_{24}, in PM80 it is *n*-C_{20}. This pattern is similar in PI. PI10 and PI30 have their second maxima at *n*-C_{26} and PI80 at *n*-C_{24}.

Short-chain *n*-alkanols from *n*-C_{15} to *n*-C_{18} are more abundant than long-chain *n*-alkanols from *n*-C_{28} to *n*-C_{34} in both bogs. *n*-C_{31} is completely absent in peat and plants, and *n*-C_{29} is only present in PM80. As already discussed above, encompass PM30 and PI30 only small amounts of *n*-alkanols, whereas peat samples in 10cm and 80cm show similar concentrations.

n-alkanols in *Calluna vulgaris* and *Sphagnum* ssp. range from *n*-C_{20} to *n*-C_{32}. *Sphagnum* has its first maximum at *n*-C_{24} and its second at *n*-C_{26}. *Calluna* peaks at *n*-C_{22} and at *n*-C_{24}.

3.4. Terpenoids

3.4.1. Tetracyclic triterpenoids: Steroids

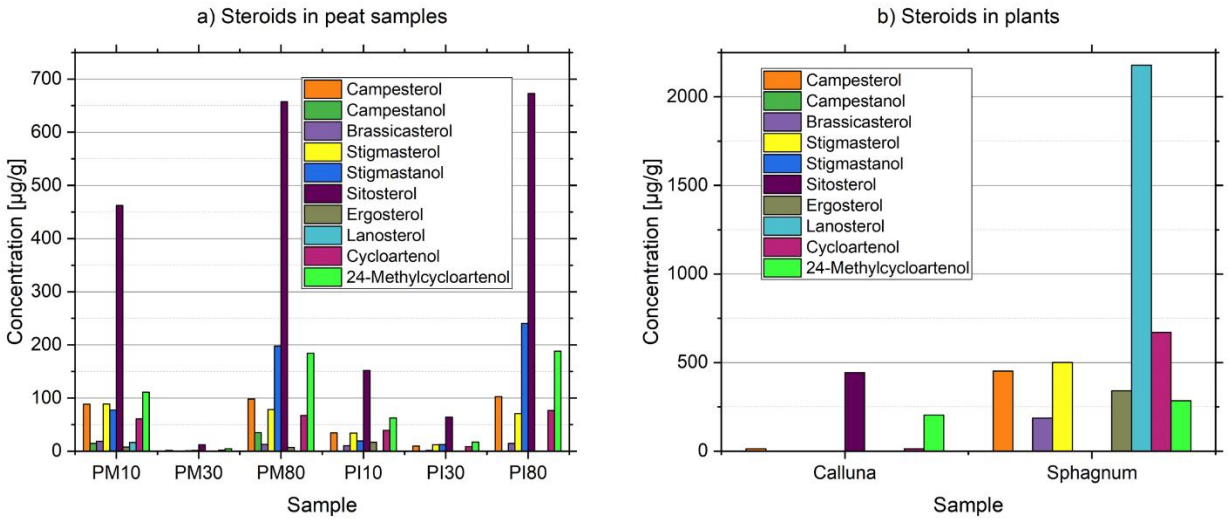

Figure 15 Relative abundance [µg/g] of each steroid molecule (lanosterol, ergosterol, sitosterol, stigmastanol, stigmasterol, brassicasterol, campesterol and campestanol) detected in (a) the peat samples of PM and PI and (b) the plant samples Calluna and Sphagnum. Legend below the graphs.

Figure 15a and b depicts the distribution of steroids detected in the peat samples (a) and plant samples (b).

In peat samples, the by far most abundant molecule identified is sitosterol, followed by stigmasterol and its degradation product stigmastanol and brassicasterol. PM shows higher values in 10cm depth (462µg/g) than PI10 (152µg/g), whereas concentration is slightly higher in PI30 than in PM30 (64µg/g and 12µg/g).

Campestanol is abundant in PM, namely in PM10 (15µg/g) and PM30 (35µg/g). Ergosterol is present in all samples of PM. It decreases from 10cm to 30cm from 8µg/g to 0,3µg/g until the concentration increases again in PM80 to 7µg/g. In PI, ergosterol was only found in the upper two samples. It also decreases from 10cm to 30cm. PI10 contained 17µg/g, PI30 just 0,2µg/g.

Steroid variety is low in *Calluna vulgaris*. Sitosterol is the most abundant steroid (443µg/g), followed by 204µg/g of 24-methylcycloartenol. Further, the sample contained 14µg/g of cycloartenol and 13µg/g of campesterol (Fig. 15b).

Instead of sitosterol, the by far most abundant molecule in the *Sphagnum* biomass sample is lanosterol with 2178µg/g, followed by cycloartenol 670µg/g, stigmasterol with 501,7µg/g, campesterol with 452,3µg/g, ergosterol with 341,3µg/g, 24-methylcycloartenol with 285µg/g, and finally brassicasterol 187,2µg/g (Fig. 15b). Among the peat samples, lanosterol was solely detected in PM in 10cm depth.

3.4.2. Pentacyclic Triterpenoids

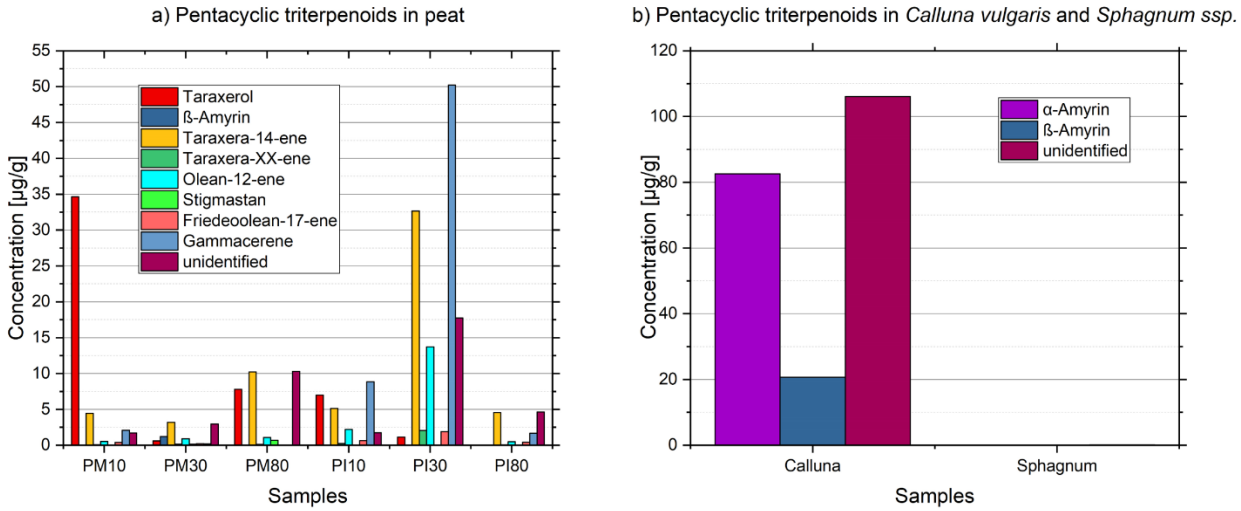

Figure 16 Relative abundance [µg/g] of each pentacyclic triterpenoid molecule (Taraxerol, Taraxera-XX-ene, etc.) detected in (a) the peat samples of PM and PI and (b) the plant samples Calluna and Sphagnum. Legend of the molecules below the graph.

The identified pentacyclic triterpenoids include the two alcohols β-amyrin and taraxerol, as well as the chiefly unsaturated molecules that are typically found in vascular plants, such as taraxera-14-ene, taraxera-XX-ene (tentatively identified), olea*n*-12-ene, stigmastane,

frideoolea*n*-17-ene, and gammacerene (Fig. 16a). Each sample contained pentacyclic triterpenoids that could not be clearly assigned to a molecule. They all showed characteristic peaks at m/z 191, but no corresponding molecule was found in literature or in NIST.

The distribution of the individual triterpenoids in peat varies greatly between the samples and through each peat core. Although PI30 contains the highest amount of pentacyclic triterpenoids and PM30 the least (Fig. 16a), the relative abundance (table 2) exhibits the same depth trend.

Taraxera-14-ene and taraxerol are the most abundant components in PM10 (4µg/g and 35µg/g) and PM80 (10µg/g and 8µg/g). In PM30, β-amyrin and taraxera-14-ene values are highest (1,2µg/g and 0,2µg/g).

PI10 exhibits maxima at taraxera-14-ene, taraxerol, and gammacerene (5µg/g, 7µg/g and 9µg/g). In PI30, 50µg/g of gammacerene were detected, followed by 33µg/g taraxera-14-ene, and 14µg/g olea*n*-12-ene. PI80 was dominated by 5µg/g of taraxera-14-ene. Taraxera-XX-ene and olea*n*-12-ene could be detected in every peat sample but in comparably low concentrations. Friedeoolea*n*-17-ene is also found in every peat sample but PM80. Stigmastane is only present in PM30 and PM80 in very small concentrations of 0,2µg/g and 0,7µg/g.

Apart from PM30, β-amyrin was only detected in *Calluna* with 20,7µg/g. α-amyrin is completely missing in all peat samples but comprises 83µg/g in *Calluna* (Fig. 16b).

Sphagnum did not contain any pentacyclic triterpenoids.

3.4.3. Hopanoids + Archaeol

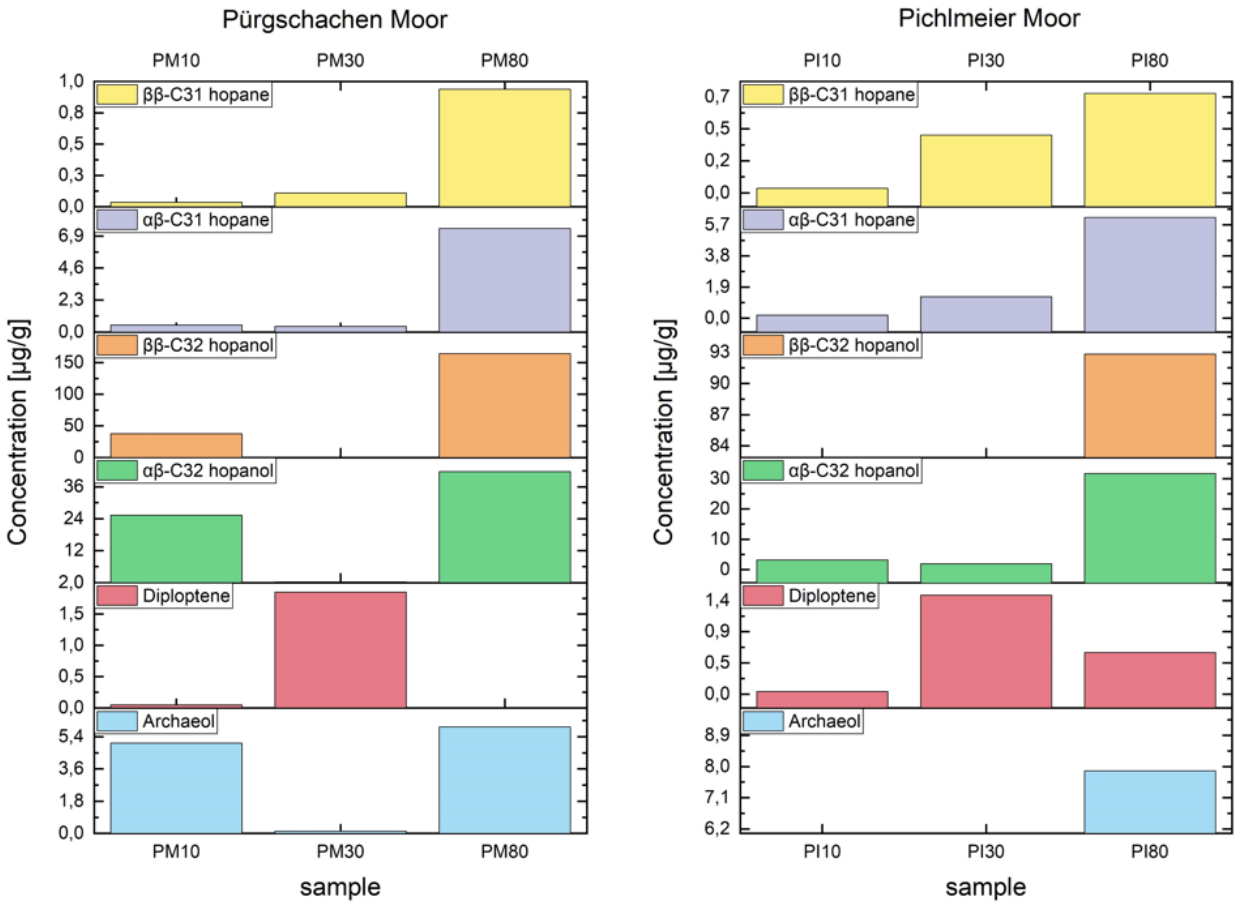

Figure 17 Concentrations [µg/g] of hopanoids and archaeol detected in peat samples in 10cm, 30cm and 80cm depth in Pürgschachen Moor (left) and Pichlmeier Moor (right).

Figure 17 displays the distribution patterns of hopanoids and archaeol found in the peat cores. Besides diploptene, the two stereoisomers of C_{32}-hopanol and those of C_{31}-hopane were identified.

All hopanoids and archaeol, except diploptene, exhibit a clear maximum at 80cm depth in both PM and PI. Diploptene in contrast is most abundant with 1,49µg/g and 1,85µg/g in PI and PM.

Concerning concentrations, the overall most abundant component is 17β(H),21β(H)-32-hopanol. It is present in all layers in PM. In 10cm 37,6µg/g are found, in 30cm it decreases to 0,2µg/g until it increases strongly to 164,1µg/g in 80cm depth. In PI, only in 80cm a concentration of 92,8µg/g was identified.

The concentrations of its isomer 17α(H),21β(H)-32-hopanol are 41,7µg/g and 31,7µg/g in PM80 and PI80, 25,3µg/g and 3,1µg/g in PM10 and PI10. PM30 and PI30 contained 0,3µg/g and 1,9µg/g.

17β(H),21β(H)-31-hopane was not present in 10cm depth. Values are increasing from PM30 and PI30 (0,1µg/g and 0,4µg/g) to PM80 and PI80 (0,9µg/g and 0,7µg/g).

17α(H),21β(H)-homohopane was observed in all samples. In PM80 and PI80 7,4µg/g and 6,1µg/g, in PM10 and PI10 0,5µg/g and 0,2µg/g. PM30 and PI30 contain 0,4µg/g and 1,3µg/g. αβ-C32 hopanol exhibits notable variations in concentration, with the highest levels observed in PM80 (41.7 µg/g) and PI80 (31.7 µg/g). Smaller quantities are also detected at other depths, indicating a wider distribution.

The terpenoid archaeol is present in all samples of PM. It shows high abundances in PM10 and PM80 (5µg/g and 6µg/g), but only marginal amounts in PM30 (0,1µg/g). In PI, archaeol was only detectable in 80cm depth with 7,9µg/g.

In Calluna, no pentacyclic terpenoids nor archaeol were identified. *Sphagnum* contained only 0,12µg/g diploptene.

3.5. Indices

3.5.1. Carbon Preference Index and Average Chain Length

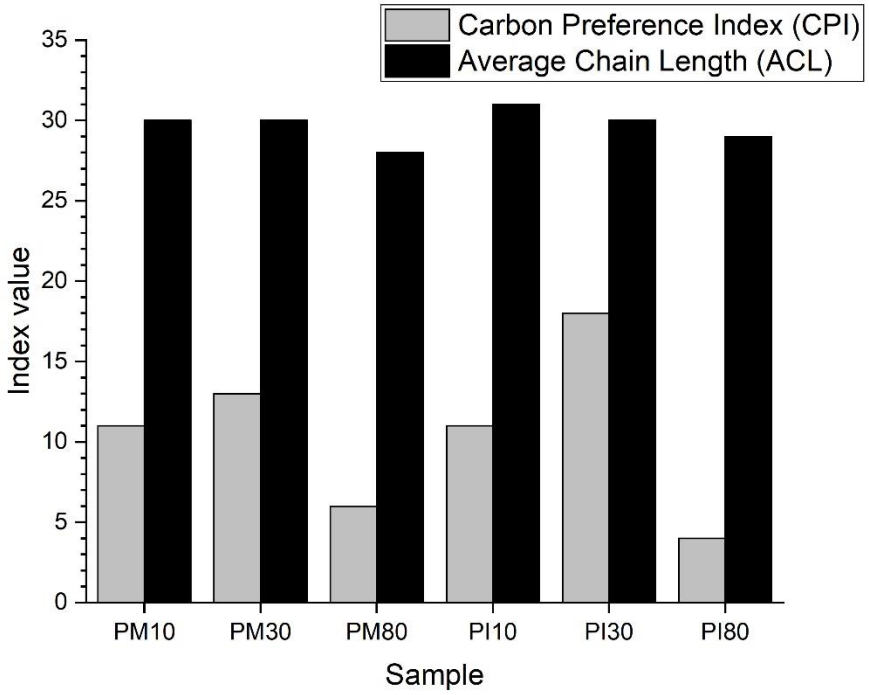

Figure 18 Carbon Preference Index and Average Chain *Length results for each peat sample in PM and PI (for CPI and ACL formula, see section 2.5)*

As all indices based on *n*-alkanes reflect the source and degree of decomposition of organic matter, they were only calculated for the peat samples (Figures 18).

The CPI patterns show the same trends in both bogs. Values increase from 10cm (11 in PM and PI) to 30cm (13 in PM and 18 in PI) until they strongly decrease in 80cm depth (6 in PM and 4 in PI) (Fig. 2).

As with the CPI, both bogs exhibit a downwards trend of ACL values. The highest ACL is found in 10cm depth (30 in PM and 31 in PI), in PI the value decreases in 31cm to 30, whereas in PM the value remains at 30. The lowest values were calculated for 80cm depth. In PM, ACL is 28 and in PI it is at 29.

3.5.2. Paq and vegetation ratios

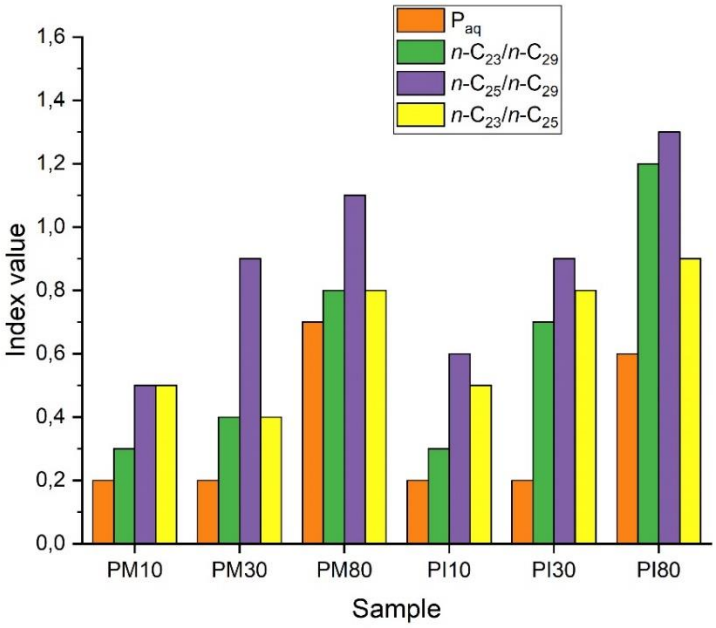

Figure 19 Results of the calculated P_{aq} index, and n-C_{23}/n-C_{29}, n-C_{25}/n-C_{29}, and n-C_{23}/n-C_{25} ratios of each peat sample of PM and PI

Figure 19 shows the calculated values for the P_{aq} index and the ratios of *n*-C_{23}/*n*-C_{29}, *n*-C_{25}/*n*-C_{29}, and *n*-C_{23}/*n*-C_{25}. As described above, *n*-C_{23} represents a common chain length in *Sphagnum* species favouring humid conditions, and *n*-C_{25} *Sphagnum* species in drier environments. *n*-C_{29} is used as an indicator for vascular plants. The ratios provide insights into the relative proportions of specific *n*-alkane chain lengths.

Except for the *n*-C_{23}/*n*-C_{25} ratio, are all values increasing with depth in both PM and PI.

The P_{aq} values augment from 0,3 to 0,4 and to 0,8 in PM and from 0,3 to 0,4 and to 1,2 in PI. *n*-C_{23}/*n*-C_{29} ratio. The *Sphagnum* vs. vascular plant ratios *n*-C_{23}/*n*-C_{29} and *n*-C_{25}/*n*-C_{29} range from 0,3 to 0,8 in PM and from 0,5 to 1,1 in PI for the first ratio. The latter also increases from 0,5 to 0,9 and to 1,1 in PM, and from 0,6 to 0,9 and to 1,3.

Only the *Sphagnum* species ratio *n*-C_{23}/*n*-C_{25} develops differently in the two bogs. Overall, they both increase with depth, but in PM30 the value decreases from 0,5 (PM10) to 0,4 (PM30) until it increases up to 0,9 (PM80). In PI, the ratio steadily increases 0,5 (PI10) to 0,8 (PI30) and 0,9 (PI80) from a more *n*-C_{25} dominated peat to a bigger contribution of *n*-C_{23}.

4. Discussion

In this section, the previously presented results will be discussed in order to answer the research questions.

4.1. Plant biomarkers

4.1.1. *n*-alkanes

Generally, total *n*-alkane concentrations in peat samples are relatively low (He et al., 2019; Ficken et al., 1998), but similar amounts were found in peatlands from lower mean annual temperature like tundra or taiga (Serebrennikova et al., 2018). *n*-alkane distribution in all peat samples ranged from C_{15} to C_{33} with a strong odd over even predominance between C_{21} and C_{33}. The most abundant *n*-alkanes are odd mid- and long-chain *n*-alkanes from C_{23} to C_{33}. The distribution clearly shows a dominant input of vascular plants and *Sphagnum* mosses.

This distribution pattern in peat aligns with the dominating *n*-alkanes found in species inhabiting both peat bogs. For example, *Rhynchospora alba* and the leaves of *Calluna vulgaris* synthesize high amounts of *n*-C_{31}, *Molinia caerulea* or the stem of *Calluna* exhibit peaks at *n*-C_{29}, or *Drosera sp.* at *n*-C_{27} (Ortiz et al., 2011). As mentioned above, *Sphagnum* species have high concentrations at *n*-C_{23} and *n*-C_{25}, but also at *n*-C_{31} or *n*-C_{33} (Baas et al., 2000). Also, the *Calluna* biomass sample shows characteristics *n*-alkane peaks for vascular plants at C_{29}, C_{31} and C_{33}.

n-alkane concentrations in the *Sphagnum* biomass sample are relatively low compared to Pancost et al. (2002) and Ficken et al. (1998). The *n*-alkane distribution in *Sphagnum* biomass sample exhibits most abundant peaks at *n*-C_{31} and *n*-C_{33} with high concentrations at *n*-C_{25} and *n*-C_{23}. The dominance of four peaks indicates that the *Sphagnum* sample consists of several *Sphagnum* species.

The results of the *n*-C_{23}/*n*-C_{25} ratio indicate a higher contribution of *Sphagna* preferring drier conditions in PM10, PM30, and PI10. According to Bingham et al. (2010), *S. magellanicum*, S. fuscum, *S. rubellum* peak at *n*-C_{25} and favour more aerated sites. Downcore, there is no clear predominance of either *n*-C_{23} or *n*-C_{25}. This suggests that the contribution of the humid-

favouring species increases with depth. Species with dominant *n*-C_{23} concentrations are S. angustifolium and *S. cupsidatum* (Bingham et al., 2000; Pancost et al., 2002). All of these species are present in PM and PI.

4.1.2. ACL, Paq and plant ratios

The downcore decrease of the ACL in both PM and PI would suggest a change in species composition (table 2). The higher ACL in the upper layers index accounts for drier conditions, whereas the lower values downcore indicate a slightly wetter environment (Bhattacharya et al., 2021). Still, it is important to again emphasize that the ACL is no standardized index and merely suggests trends.

Nevertheless, increasing P_{aq} value, and *n*-C_{23}/*n*-C_{29}, and *n*-C_{25}/*n*-C_{29} ratios also indicate an elevated contribution of wetland plants compared to vascular plants with depth. This suggests wetter conditions downcore in both bogs. *n*-C_{23}/*n*-C_{29}, and *n*-C_{25}/*n*-C_{29} ratios show that at 80cm depth, the input of mosses even dominates over vascular plant input.

4.1.3. Steroids and plant derived pentacyclic triterpenoids

The relative distribution of steroids and plant derived pentacyclic triterpenoids changes with depth. Steroid abundance is highest in 10cm and 80cm in both bogs. Pentacyclic triterpenoids are highest in 30cm depth, where steroids show lower concentrations.

Although steroids can be found in both vascular plants and *Sphagnum*, the prevalence of pentacyclic triterpenoids in *Sphagnum* mosses is scarce as they don't need epicuticular leaf waxes. The *Calluna* and *Sphagnum* biomass samples confirm this.

The steroid variety in *Calluna* is low, only sitosterol is found in small concentrations, whereas the sample is rich in pentacyclic steroids. In contrast, *Sphagnum* exhibits no pentacyclic triterpenoids but is very rich in steroid content and variety.

This distribution would indicate a generally higher contribution of *Sphagnum* to the peat body of 10cm and 80cm depth in both bogs. Only in 30cm vascular plant species contribution seems to be elevated.

Nevertheless, the *Sphagnum* biomass sample shows some peculiarities. Although sitosterol is described to be the dominant sterols in *Sphagnum* (Baas et al., 2000), the by far most abundant molecule identified in the *Sphagnum* biomass sample is lanosterol, while sitosterol is missing completely. Lanosterol was also detected in PM in 10cm depth. The *Sphagnum* biomass sample was extracted in the same area where the peat core PM was sampled.

Lanosterol and cycloartenol are two precursor molecules of sterols. While cycloartenol is mainly synthesized by plants or algae, lanosterol is produced by fungi or animals (Peters et al., 2004). In fungi, lanosterol is commonly degraded to ergosterol. As ergosterol was identified in both *Sphagnum* and PM10, the detected lanosterol might derive from fungi.

4.1.4. Peat composition

In the upper two layers, *n*-alkane distributions, ACL, P_{aq}, *n*-C_{23}/*n*-C_{29}, *n*-C_{25}/*n*-C_{29} ratios and the relative contribution of steroids to pentacyclic triterpenoids suggest a slightly higher contribution of higher terrestrial plants to the lipids of the peat body. Further down, species composition seems to shift towards a greater input of *Sphagnum* ssp. compared to vascular plants with depth. Both bogs exhibit the same trends.

Furthermore, the contributing *Sphagnum* species seem to change according to *n*-C_{23}/*n*-C_{25} ratio. In the upper layers, *Sphagnum* species favouring drier conditions are dominating. Further down, the abundance of species preferring humid environments increases and both groups contribute almost equally to the peat body.

These findings are in line with Drollinger et al. (2020) and Moorschutzverein Pürgschachen (2005). They observed that the main peat-forming species in PM and PI down 5,5m is *Sphagnum* moss with minor inputs of *Eriophorum* tissue. Thus, a change between emergent and submerged plant input should not be expected.

4.2. *n*-alkanols

The *n*-alkanol distribution found in this study from predominantly *n*-C_{22} to *n*-C_{26} would align with *n*-alkanols observed in *Sphagnum* mosses by Baas et al. (2000).

Further, the *n*-alkanol distributions are similar to the Hani peat in He et al. (2010). Nevertheless, He et al. (2019) found no correlation with vegetation. As *n*-alkanols can be of biochemical or

geochemical origin, source organisms are difficult to identify. For example, *n*-C_{16} to *n*-C_{24} can originate from algae or bacteria, *n*-C_{22} to *n*-C_{24} from submerged plants and *n*-C_{22} to *n*-C_{28} from submerged plants emergent or higher plants. But Naafs et al. (2019) suggest that *n*-alkanol distribution varies greatly within single plant individuals. Further, *n*-alkanols are less recalcitrant than *n*-alkanols and therefore preferentially degraded by microorganisms (Zhou et al., 2010).

Due to these manifold sources of *n*-alkanol homologues interpretations of their origin are vague (Andersson et al., 2012).

4.3. Microbial biomarkers

4.3.1. Archaeol

Archaeol is a biomarker for many archaea, but especially anaerobic methanogenic archaea are known to produce significant amounts of archaeol. Methanogenic archaea require anoxic conditions, which are abundant below the water surface. In all peatlands examined by Pancost et al. (2011), archaeol was lacking in the surface layer, but emerged somewhere between the maximum and minimum of the summer water table depth and further down.

Unfortunately, WTD data with seasonal resolution are missing for both PI and PM. As data for maximum and minimum annual WTD are available for both bogs, archaeol abundance will be compared with this data.

In PM, archaeol is abundant in moderate amounts at 10cm and 80cm depth (concentrations compared to peat bogs in Finland, Germany, Ireland, and Great Britian analysed by Pancost et al., 2011). The maximum WTD in PM lies by approximately 4cm (Drollinger et al., 2019) which creates the anoxic conditions for archaea. Surprisingly, at 30cm depth, only 0,1µg/g of archaeol were detected which is considered below detection limit at Pancost et al. (2011).

In PI, archaeol was only detectable in 80cm depth with 7,9µg/g. The maximum WTD lies around 25cm and the minimum WTD at 43cm to 56cm (Moorschutzverein Pürgschachen, 2005; Drollinger et al., 2019). The extended acrotelm in PI compared to PM doesn't provide the

anaerobic condition where archaea can thrive. The abundances of archaeol are therefore in line with the oxic and anoxic conditions of each bog.

Still, the water table does not explain why archaeol is absent at 30cm depth in PM. In both peatlands, the peat layer in 30cm depth shows extremely low concentrations of all analysed lipids compared to 10cm and 80cm.

4.3.2. Biohopanoids

The high abundance of 17β,21β(H)-C_{31}-hopane in the 10cm layers in both peatlands could be linked to the presence of aerobic methanotrophic bacteria.

In a study of Raghoebarsing et al. (2005), one of their precursor molecules bishomohopanoic acid was present in the *Sphagnum* samples. They assign this molecule to the presence of aerobic methanotrophs as they are known to live in symbiosis with the mosses. The bacteria recycle CH_4 that was produced in the anoxic catotelm and in turn provide *Sphagnum* with carbon. As they are dependent on the presence of CH_4, they prefer wetter conditions (Op den Camp et al., 2010).

Especially *S. cupsidatum* and to a lower extent *S. magellanicum* and *S. papillosum* which are found on PM and PI (Moorschutzverein Pürgschachen, 2005) seem to be inhabited by those bacteria. Therefore, the abundance of the 17β,21β(H)-C_{31}-hopane in the upper layers could indicate the presence of aerobic methanotrophs. Even so, 17β,21β(H)-C_{31}-hopane is produced by many bacteria.

Further, concentrations of the biogenic hopanoids 17β(H),21β(H)-32-hopanol and 17β,21β(H)-C_{31}-hopane are by far highest in 80cm depth in the anoxic catotelm in both bogs. are predominantly produced by aerobic bacteria. To resolve this, further investigation in the precursor molecule BHP would be advisable.

4.4. Geohopanoids

Surprisingly, the geological isomer 17α(H),21β(H)-homohopane is abundant already at 10cm depth in both PM and PI and increases with depth, suggesting an early isomerisation of the biologically derived 17β,21β(H)-homohopane by diagenesis (Inglis et al., 2018). The

concentration of 17α(H),21β(H)-homohopane in all peat samples even exceeds the one of 17β,21β(H)-homohopane by far.

This trend has been observed in ombrotrophic peatlands in all climatic zones (e.g., Pancost et al., 2003; Inglis et al., 2018; Naafs et al., 2019). The dominance of the αβ-isomer seems to correlate strongly in acidic peat bogs with a pH<6 (Inglis et al., 2018; Naafs et al., 2019). Furthermore, the presence of *Sphagnum* mosses appears to enhance the isomerisation of the αβ-C_{31} hopane where it was found to be synthesized in higher abundances. Nevertheless, acidity seems to be the major control of the catalysation as it is also abundant in peatlands, where *Sphagnum* is lacking (Inglis et al., 2018).

4.5. CPI

The results of the CPI are similar in both bogs. They suggest the highest decomposition of peat in 80cm depth, well-preserved organic matter in 30cm and slightly altered organic matter in the top 10cm.

Though the CPI patterns are similar in both bogs, they have a different hydrology (table 1). Whereas PM10 is expected to reflect the boundary of acrotelm and catotelm, PM30 and PM80 should already be in the catotelm. Sample PI10 derives from the aerobic acrotelm, P30 represents the acrotelm/catotelm interface and only PI80 is permanently waterlogged. Thus, since both CPI values are similar, they seem to be decoupled from the water table depth. This finding and decomposition trend is surprising when comparing it to the conclusions of Drollinger et al. (2020). But this will be discussed in detail below.

With less available energy sources for decomposers, degree of degradation would be expected to be low in the catotelm and high in the acrotelm/catotelm boundary, where oxygen and labile carbon is abundant (Reddy and DeLaune, 2008).

Unfortunately, no similar data has been found in literature. For example, the fen and peat bog examined by Lehtonen and Ketola (1993) showed an increase of CPI with depth, hence better preservation. Although, it must be noted that they did not declare which CPI formula they used. Andersson et al. (2012) obtained a similar pattern for CPI of the *n*-alkanes with lowest CPI values

in depth from a peat bog in the Siberian tundra and taiga but with completely different vegetation and high fen deposit.

4.6. Decomposition

The low downcore CPI values suggest high microbial activity.

In this study, all microbial lipid biomarkers exhibit highest concentrations in 80cm depth in both PM and PI (table 6), only diploptene was not following this trend.

In contrast, concentrations of the microbial biomarkers are either lowest, or the compounds entirely absent in 10cm and 30cm depth. This supports the results of the CPI.

The high CPI in 30cm is suggesting well preserved organic matter. Diploptene is most abundant in 30cm in PI and PM (Fig. 17). According to Bhattacharya et al. (2021), the presence of diploptene implies a low degree of decomposition. Diploptene can be synthesized directly by both anaerobic and aerobic bacteria (López-Días et al., 2010; Inglis et al., 2018). Although high concentrations of bacterial products could indicate high microbial activity in this peat layer, Bhattacharya et al. (2021) propose that diploptene reflects rather anoxic conditions during deposition. To identify the species producing diploptene, further analysis would be necessary.

4.6.1. Comparison of decomposition trends

Although the results of vegetation and peat composition align with the findings of Drollinger et al. (2019) and Drollinger et al. (2020), CPI values and the abundance of microbial biomarkers show a differing trend in post-depositional alteration.

In their paper, Drollinger et al. (2020) apply several proxies that show signs of secondary decomposition in both PM and PI. The found that degree of degradation increases downcore from the surface until it reaches its highest values between 40-60cm depth. After 60cm, decomposition decreases strongly. This is in strong contrast to CPI which shows an inverse trend where degradation is highest at 80cm depth and lowest in 30cm, and slightly higher in 10cm (Fig. 18).

For their analysis, Drollinger et al. (2020) took several peat cores in each PM and PI and grouped them to classes of expected degradation status. Four samples were extracted in the same area

of the open peat bog in PM, where also the core for this study originates from. In PI, the sampling sites differed from the one of this study. Thus, values can only be compared for PM.

After analysing amongst others C/N ratio and bulk density, Drollinger et al. (2020) calculated the mean values of each parameter for these four samples, resulting in the decomposition pattern described above.

Nevertheless, when looking into the data in the appendix, two of these four samples exhibit the same decomposition trend as examined in this study. Although all four share almost identical hydrological conditions and chemical composition, dominant vascular plant species cover diverged completely.

The two sampling sites where the decomposition pattern is in line with this study are covered with either *Rhynchospora alba* and *Eriophorum vaginatum* or *Calluna vulgaris*. But the other two sites are dominated by *Pinus mugo*.

As water table depth does not differ between these sites, secondary decomposition or re-exposition of the catotelm to air caused by alterations of the WTD might not explain this depth trend in PM.

This similar depth trend at the *Calluna* and graminoid sites would support the finding of the CPI degradation pattern. Also, Zeh et al. (2020) recently proposed that the degree of peat decomposition in their study was more affected by vascular plants growth than by hydrological changes and temperature. Therefore, the vegetation cover, especially the recent vascular input might be a major driver of this degradation depth trend of the sample PM.

4.7. Peculiarities in 30cm depth

In both, PM and PI, the lipids in 30cm depth display some peculiarities compared with those in 10cm and 80cm. Measured steroids, pentacyclic terpenoids, hopanoids, and *n*-alkanols show distinctively lower concentrations in 30cm depth compared to the other two layers. The only exception are the *n*-alkane concentrations, which are marginally higher in 30cm, although *n*-alkane concentrations are generally low.

Considering *n*-alkane CPI values, peat seems to be freshest and least altered in 30cm. Aerobic bacterial biomarkers 17β,21β(H)-bishomohopanol and 17α(H),21β(H)-bishomohopanol values are as well lowest, such as the anaerobic archaeal marker archaeol. Diploptene is highest.

Only 17β(H),21β(H)-homohopane content is intermediately high in 30cm in both bogs, 17α(H),21β(H)-homohopane only in PI. At the same time, vegetation markers such as ACL or P_{aq} are developing gradually with depth, species composition seems to be consistent. Also, there was no visually noticeable root input in 30cm depth.

As this trend appears in both bogs, recent hydrological conditions might not explain this phenomenon, as well as vegetation composition might not.

Ficken et al. (1998) describe a similar trend in their peat samples. Between 20-40cm, *n*-alkanols but also *n*-alkanes suddenly decrease, whereas *n*-alkanoic acids increase strongly. They conjecture either a change in dominant plant input or changing level of diagenesis.

As a change in species composition is not observed in this study, diagenetic processes might occur. But since this trend appears in both bogs which have different water table levels, it might be rather related to conditions during deposition, which are preserved in this specific layer.

With an average peat accumulation rate of 0,69mm yr-1 (Drollinger et al., 2020), the samples would then be approximately 70 years old in 10cm depth, 210 years in 30cm, and around 550 years in 80cm. The peat in 30cm might therefore be deposited at the end of the little Ice Age that had is last minimum (Dalto*n*-Minimum) between 1790 and 1830 BP (International Astronomical Union, n.d.a.; Büntgen et al., 2011).

5. Conclusion

This study conducted lipid biomarker analysis on cores of two different peatlands with diverging degradation history to infer species composition and signs of secondary decomposition.

Overall, biomarker distribution was similar in both peatlands. The same species plant species composition was detected but also decomposition patterns and similar microbial activity.

n-alkane distribution provides insight into peat species composition. Various indices based on n-alkanes like the ACL or the P_{aq} and steroid/pentacyclic triterpenoid contributions indicated input of vascular plants and *Sphagnum* in all peat layers which is in line with vegetation surveys of both peatlands. The species composition seems to change downcore to a more *Sphagnum* dominated peat body which also aligns with Drollinger et al. (2020).

It is important to emphasise that plant biomarkers are often interpreted as indicators of rather depositional conditions than post depositional alterations. Even so, they merely provide information about the current constitution of biomarkers. The question remains open whether *Sphagnum* species are dominant downcore due to different past climatic conditions, meaning that there was no or only little vascular plant growth, or due to better recalcitrance of *Sphagnum* to microbial degradation. Latter was already indicated by Karunen and Ekman (1982), Broder et al. (2012) and Andersson et al., (2012a).

CPI showed no clear signs of secondary decomposition in neither bog and could therefore not confirm the findings of Drollinger et al. (2020) and Drollinger et al. (2019). In contrast, the results suggested an inverse decomposition trend, where the degree of decomposition is highest in 80cm depth and organic matter is best preserved in 30cm depth. As this trend is observed in both bogs with differing water table depth, hydrology might not exert the major control.

The results of CPI were supported by high abundance of microbial biomarkers in 80cm and their absence in 30cm depth. The only microbial biomarker detected in 30cm depth was diploptene. Although diploptene can be synthesized by various aerobic and anaerobic bacteria,

Bhattacharya et al. (2021) found diploptene in peat to be assigned with fresh plant material. In all layers on the other hand, diploptene was identified only in small amounts.

The presence of archaeol in 80cm depth is attributed to the activity of anaerobic methanogenic archaea below the water table. Also, in PM10 high concentrations of archaeol were detected, indicating a high water table. Nevertheless, it is curious that archaeol is completely missing in PM30. In PI, the presence of archaeol aligns with the water table depth.

Biogenic hopanoids in the upper layers in PM and PI imply the activity of aerobic methanotrophic bacteria living in symbiosis with *Sphagnum* mosses. They are found to inhabit S. cupsidatum and S. magellanicum that are also present in both bogs.

In both peatlands, the sample at 30cm showed some peculiarities, for example relatively low concentrations in lipids but well preserved organic matter (high CPI) or low microbial activity. As this occurs in both bogs, this might either be a coincidence or due to climatic circumstances. A higher sampling resolution and further analysis such as characterization of BHPs or isotopic biomarker signature could get a more comprehensive insight into recent and past processes.

While some differences in molecular distributions occur between the bogs, there are no distinct differences in general trends of peat composition, degree of decomposition and microbial activity. The findings were quite in line with water table data. This resemblance might source in the fact that the sample in PI was extracted at a site considered as capable for regeneration.

Although no distinctive plant specific biomarkers exist, *Sphagnum* ssp. seems to play a crucial role in lipid biomarker distribution in all depths and in (methanotrophic) microbial activity. Even in 80cm depth, n-alkanes assigned to *Sphagnum* could be determined. These findings indicate that the re-establishment of typical peat bog vegetation is crucial for restoring the carbon sink function.

6. Acknowledgements

I would have never guessed that writing this thesis would be such a long endeavour. In the past year, I learned so much, also about myself. There were so many people on my side helping and believing me, which I am so grateful for.

First of all, I want to thank my supervisor, Stephan Glatzel, for supporting me from day one when I came to his office expressing my interest in a master thesis in geoecology. Thank you for giving me the opportunity to be part of the geoecology working group and for believing in me, even though I have a different academic background.

I'd also like to thank Beatrix Bethke, not only for teaching me how to extract lipids. Thank you so much for all your help, patience, and encouragement. I really enjoyed working with you in the lab and our talks at coffee breaks.

Further, a special thanks to Daniel Birgel who just out of the blue agreed to deal with me and my samples for three whole weeks. I am so grateful that I had the opportunity to come to Hamburg and learn from you.

Of course, I want to thank my mother and grandmother, who always supported me my whole life without ever questioning me. Thank you so much for genuinely wanting the best for me.

Finally, I want to express my gratitude to Michi, the guru next door who always supplied me with his kindness and sometimes really bad jokes.

7. Literature

Amt der Steiermärkischen Landesregierung. Natura 2000: Europaschutzgebiet Pürgschachen Moos. Fachabteilung 13C Naturschutz, Ziviltechnikkanzlei Dr. Hugo Kofler. URL: https://www.natura2000.steiermark.at/cms/dokumente/12596370_138816479/a16de02e/P%C3%BCrgschachen-Moos-2.pdf

Amt der Steiermärkischen Landesregierung, Ziviltechnikkanzlei Dr Kofler (2006): Managementplan Europaschutzgebiet „Pürgschachen-Moos“. Kurzfassung. URL: https://www.verwaltung.steiermark.at/cms/dokumente/11680781_74835791/db4c63d3/Puergschachen%20Moos%20MP%20Kurzfassung%203.pdf

Andersson, R. A., Meyers, P., Hornibrook, E., Kuhry, P., Mörth, C.-M. (2012a). Elemental and isotopic carbon and nitrogen records of organic matter accumulation in a Holocene permafrost peat sequence in the East European Russian Arctic. Journal of Quaternary Science, 27(6), 545–552. doi: 10.1002/jqs.2541

Andersson, R. A., Meyers, P. A. (2012). Effect of climate change on delivery and degradation of lipid biomarkers in a Holocene peat sequence in the Eastern European Russian Arctic. Organic Geochemistry, 53, 63–72. doi: 10.1016/j.orggeochem.2012.05.002

Baas, M., Pancost, R., Van Geel, B., Sinninghe Damste, J. S. (2000). A comparative study of lipids in *Sphagnum* species. Organic Geochemistry, 31(6), 535–541. doi: 10.1016/S0146-6380(00)00037-1

Beer, J., Lee, K., Whiticar, M., Blodau, C. (2008): Geochemical Controls on AnaerobicOrganic Matter Decomposition in a Northern Peatland. Limnology and Oceanography. 53(4). 1393–1407. DOI: https://doi.org/10.4319/lo.2008.53.4.1393

Berdié, L., Grimalt, J. O., Gjessing, E. T. (1995). Hydrocarbons, alcohols and strols in the dissolved + colloidal and particulate phases of the waters from a dystrophic lake, Skjervatjern Lake (Norway). Water Research (Oxford), 29(9), 2017–2030. doi: 10.1016/0043-1354(95)00028-J

Bhattacharya, S., Kishor, H., Ankit, Y., Mishra, P. K., Srivastava, P. (2021). Vegetation History in a Peat Succession Over the Past 8,000 years in the ISM-Controlled Kedarnath Region, Garhwal Himalaya: Reconstruction Using Molecular Fossils. Frontiers in Earth Science (Lausanne), 9. doi: 10.3389/feart.2021.703362

Biester, H., Knorr, K. H., Schellekens, J., Basler, A., Hermanns, Y. M. (2014): Comparison of different methods to determine the degree of peat decomposition in peat bogs. Biogeosciences. 11(10). 2691–2707. DOI: https://doi.org/10.5194/bg-11-2691-2014

Bingham, E. M., McClymont, E. L., Väliranta, M., Mauquoy, D., Roberts, Z., Chambers, F. M., … Evershed, R. P. (2010). Conservative composition of n-alkane biomarkers in *Sphagnum* species: Implications for palaeoclimate reconstruction in ombrotrophic peat bogs. Organic Geochemistry, 41(2), 214–220. doi: 10.1016/j.orggeochem.2009.06.010

Bundesministerium für Landwirtschaft, Regionen und Tourismus (BMLRT). (2022): Moorstrategie 2030+

Borgmark, A., Schoning, K. (2006): A comparative study of peat proxies from two eastern central Swedish bogs and their relation to meteorological data. Journal of Quaternary Science. 21(2). 109–114. DOI: https://doi.org/10.1002/jqs.959

Broder, T., Blodau, C., Biester, H., Knorr, K. H. (2012): Peat decomposition records in three pristine ombrotrophic bogs in southern Patagonia. Biogeosciences. 9(4). 1479–1491. DOI: https://doi.org/10.5194/bg-9-1479-2012

Büntgen, U., Tegel, W., Nicolussi, K., McCormick, M., Frank, D., Trouet, V., … Esper, J. (2011). 2500 Years of European Climate Variability and Human Susceptibility. Science (American Association for the Advancement of Science), 331(6017), 578–582. doi: 10.1126/science.1197175

Drollinger, S., Knorr, K. H., Knierzinger, W., Glatzel, S. (2020): Peat decomposition proxies of Alpine bogs along a degradation gradient. In: Geoderma. 369

Drollinger, S., Kuzyakov, Y., Glatzel, S. (2019): Effects of peat decomposition on δ 13 C and δ 15 N depth profiles of Alpine bogs. In: CATENA. 178, p. 1-10

Drzymulska, D. (2016): Peat decomposition; shaping factors, significance in environmental studies and methods of determination - a literature review. Geologos. 22(1). 61–69. DOI: https://doi.org/10.1515/logos-2016-0005

Evans, E.D., Peacock, M., Baird, A. J., Artz, R. R. E., Burden, A., Callaghan, N., Chapman, P. J., Cooper, H. M., Coyle, M., Craig, E., Cumming, A., Dixon, S., Gauci, V., Grayson, R. P., Helfter, C., Heppell, C. M., Holden, J., Jones, D. L., Kaduk, J., … Morrison, R. (2021). Overriding water table control on managed peatland greenhouse gas emissions. Nature (London). 593(7860). 548–552O. DOI: https://doi.org/10.1038/s41586-021-03523-1

Ficken, K. J., Barber, K. E., Eglinton, G. (1998). Lipid biomarker, δ13C and plant macrofossil stratigraphy of a Scottish montane peat bog over the last two millennia. Organic Geochemistry, 28(3), 217–237. doi: 10.1016/S0146-6380(97)00126-5

Ficken, K. J., Li, B., Swain, D.,Eglinton, G. (2000). An n-alkane proxy for the sedimentary input of submerged/floating freshwater aquatic macrophytes. Organic Geochemistry, 31(7), 745–749. doi: 10.1016/S0146-6380(00)00081-4

Flores, R. (2014). Origin of Coal as Gas Source and Reservoir Rocks. In Coal and coalbed gas : fueling the future / (pp. 97–165). Waltham, MA :: Elsevier. doi: 10.1016/B978-0-12-396972-

Foti, R., del Jesus, M., Rinaldo, A., & Rodriguez-Iturbe, I. (2012). Hydroperiod regime controls the organization of plant species in wetlands. Proceedings of the National Academy of Sciences - PNAS, 109(48), 19596–19600. https://doi.org/10.1073/pnas.1218056109

Glatzel, S., Lemke, S., & Gerold, G. (2006): Short-term effects of an exceptionally hot and dry summer on decomposition of surface peat in a restored temperate bog. European Journal of Soil Biology. 42(4). 219–229. DOI: https://doi.org/10.1016/j.ejsobi.2006.03.003

Glatzel, S. (2021): Moore und Klimawandel: Intakte Moore schützen, degradierte revitalisieren. Natur. Raum. Management., 50(04). 10-11.

https://www.bundesforste.at/fileadmin/publikationen/naturraum/NRM_Journal_4_2021_screen.pdf

He, D., Huang, H., Arismendi, G. G. (2019). n-Alkane distribution in ombrotrophic peatlands from the northeastern Alberta, Canada, and its paleoclimatic implications. Palaeogeography, Palaeoclimatology, Palaeoecology, 528, 247–257. doi: 10.1016/j.palaeo.2019.05.018

Inglis, G. N., Naafs, B. D. A., Zheng, Y., McClymont, E. L., Evershed, R. P., Pancost, R. D. (2018). Distributions of geohopanoids in peat: Implications for the use of hopanoid-based proxies in natural archives. Geochimica et Cosmochimica Acta, 224, 249–261. doi: 10.1016/j.gca.2017.12.029

Killops, S. D., & Frewin, N. L. (1994). Triterpenoid diagenesis and cuticular preservation. Organic Geochemistry, 21(12), 1193–1209. doi: 10.1016/0146-6380(94)90163-5

Lehtonen, K., Ketola, M. (1993). Solvent-extractable lipids of *Sphagnum*, Carex, Bryales and Carex-Bryales peats: content and compositional features vs peat humification. Organic Geochemistry, 20(3), 363–380. https://doi.org/10.1016/0146-6380(93)90126-V

Leifeld, J., Menichetti, L. (2018): The underappreciated potential of peatlands in global climate change mitigation strategies. Nature Communications, 9(1), 1071–1077. DOI: https://doi.org/10.1038/s41467-018-03406-6

Li, X., Anderson, B. J., Vogeler, I., Schwendenmann, L. (2018). Long-chain n-alkane and n-fatty acid characteristics in plants and soil - potential to separate plant growth forms, primary and secondary grasslands? The Science of the Total Environment, 645, 1567–1578. https://doi.org/10.1016/j.scitotenv.2018.07.105

López-Días, V., Borrego, Á. G., Blanco, C. G., Arboleya, M., López-Sáez, J. A., & López-Merino, L. (2010). Biomarkers in a peat deposit in Northern Spain (Huelga de Bayas, Asturias) as proxy for climate variation. Journal of Chromatography A, 1217(21), 3538–3546. doi: 10.1016/j.chroma.2010.03.038

McMaster, M.C. (2008): GC/MS. a practical user's guide. 2nd edition. Hoboken, New Jersey: Wiley-Interscience.

Moorschutzverein Pürgschachen, Amt der Steiermärkischen Landesregierung, Ziviltechnikkanzlei Dr.Kofler (2005): Fachbericht Moore. Beilage B.3.

Mortimer, C. E., & Müller, U. (2010). Chemie (10. Auflage.). Stuttgart, Germany :: Thieme.

Naafs, B. D. A., Inglis, G. N., Blewett, J., McClymont, E. L., Lauretano, V., Xie, S., Evershed, R. P., Pancost, R. D. (2019). The potential of biomarker proxies to trace climate, vegetation, and biogeochemical processes in peat: A review. Global and Planetary Change, 179, 57–79. https://doi.org/10.1016/j.gloplacha.2019.05.006

Op den Camp, H. J. M., Kip, N., van Winden, J. F., Pan, Y., Bodrossy, L., Reichart, G.-J., … Damsté, J. S. S. (2010). Global prevalence of methane oxidation by symbiotic bacteria in peat-moss ecosystems. Nature Geoscience, 3(9), 617–621. doi: 10.1038/ngeo939

Ortiz, J. E., Borrego, A. G., Gallego, J. L. R., Sanchez-Palencia, Y., Urbanczyk, J., Torres, T., Domingo, L., Estebanez, B. (2016): Biomarkers and inorganic proxies in the paleoenvironmental reconstruction of mires; the importance of landscape in Las Conchas (Asturias, northern Spain). Organic Geochemistry, 95. 41–54. DOI: https://doi.org/10.1016/j.orggeochem.2016.02.009

Pancost, R. D., Baas, M., van Geel, B., Sinninghe Damsté, J. S. (2002). Biomarkers as proxies for plant inputs to peats: an example from a sub-boreal ombrotrophic bog. Organic Geochemistry, 33(7), 675–690. doi: 10.1016/S0146-6380(02)00048-7

Pancost, R. D., Baas, M., van Geel, B., Sinninghe Damsté, J. S. (2003). Response of an ombrotrophic bog to a regional climate event revealed by macrofossil, molecular and carbon isotopic data. Holocene (Sevenoaks), 13(6), 921–932. doi: 10.1191/0959683603hl674rp

Pancost, R. D., McClymont, E. L., Bingham, E. M., Roberts, Z., Charman, D. J., Hornibrook, E. R. C., … Evershed, R. P. (2011). Archaeol as a methanogen biomarker in

ombrotrophic bogs. Organic Geochemistry, 42(10), 1279–1287. doi: 10.1016/j.orggeochem.2011.07.003

Peters, K. E., Walters, C. C., Moldowan, J. M. (2004). The Biomarker Guide (Vol. 1). Cambridge University Press. https://doi.org/10.1017/CBO9780511524868

Philp, R. P. (1985). Fossil fuel biomarkers: applications and spectra. Amsterdam [u.a.]: Elsevier.

Raghoebarsing, A. ., Smolders, A. J. ., Schmid, M. ., Rijpstra, W. I. ., Wolters-Arts, M., Derksen, J., … Lamers, L. P. . (2005). Methanotrophic symbionts provide carbon for photosynthesis in peat bogs. Nature, 436(7054), 1153–1156. doi: 10.1038/nature03802

Rotherham, I.D. (2020): Peatlands. Milton: Taylor and Francis. DOI: 10.4324/9780429439285

Rydin, H., Jeglum, J. K., Bennett, K. D. (2013): The biology of peatlands (2nd ed.). Oxford University Press.

Samaritani, E., Siegenthaler, A., Yli-Petäys, M., Buttler, A., Christin, P.-A., Mitchell, E. A. D. (2011): Seasonal Net Ecosystem Carbon Exchange of a Regenerating Cutaway Bog: How Long Does it Take to Restore the C-Sequestration Function? Restoration Ecology. 19(4). 480–489. DOI: https://doi.org/10.1111/j.1526-100X.2010.00662.x

Schellekens, J., Bradley, J. A., Kuyper, T. W., Fraga, I., Pontevedra-Pombal, X., Vidal-Torrado, P., Abbott, G. D., Buurman, P. (2015): The use of plant-specific pyrolysis products as biomarkers in peat deposits. Quaternary Science Reviews, 123, 254–264. https://doi.org/10.1016/j.quascirev.2015.06.028

Serebrennikova, O. V., Duchko, M. A., Koronatova, N. G., Strelnikova, E. B. (2018). Concentrations and Composition of *Sphagnum* Peat Lipids Depending on Temperature in the Climatic Zones of Western Siberia. Solid Fuel Chemistry, 52(1), 36–43. doi: 10.3103/S0361521918010081

Sparkman, O.D., Penton, Z., Kitson, F. G. (2011): Gas chromatography and mass spectrometry: a practical guide. 2nd edition. Burlington, MA. Academic Press.

Wang Xinxin, Huang Xianyu, Sachse, D., Hu Yu, Xue Jiantao, Meyers, P. A. (2016): Comparisons of lipid molecular and carbon isotopic compositions in two particle-size fractions from surface peat and their implications for lipid preservation. Environmental Earth Sciences. 75(15). 1. DOI: https://doi.org/10.1007/s12665-016-5960-3

Wintereder, S. (2017): Die Vegetation des Pürgschachenmoores und ihre Entwicklung seit Beginn des 20. Jahrhunderts.

Wöstmann, R. (2007): Biomarker in torfbildenden Pflanzen und ihren Ablagerungen im nordwestdeutschen Küstenraum als Indikatoren nacheiszeitlicher Vegetationsänderungen. Carl von Ossietzky University Oldenburg. Dissertation.

Yu, Z., Loisel, J., Brosseau, D. P., Beilman, D. W., Hunt, S. J. (2010): Global peatland dynamics since the last glacial maximum. Geophysical Research Letters. 37(13). DOI: https://doi.org/10.1029/2010GL043584

Zeh, L., Igel, M. T., Schellekens, J., Limpens, J., Bragazza, L., Kalbitz, K. (2020). Vascular plants affect properties and decomposition of moss-dominated peat, particularly at elevated temperatures. Biogeosciences, 17(19), 4797–4813. doi: 10.5194/bg-17-4797-2020

Zhang, Y., Meyers, P. A., Liu, X., Wang, G., Ma, X., Li, X., … Wen, B. (2016). Holocene climate changes in the central Asia mountain region inferred from a peat sequence from the Altai Mountains, Xinjiang, northwestern China. Quaternary Science Reviews, 152, 19–30. doi: 10.1016/j.quascirev.2016.09.016

Zhou, W., Zheng, Y., Meyers, P. A., Jull, A. J. T., Xie, S. (2010). Postglacial climate-change record in biomarker lipid compositions of the Hani peat sequence, Northeastern China. Earth and Planetary Science Letters, 294(1), 37–46. doi: 10.1016/j.epsl.2010.02.035

International Astronomical Union (07/08/2015): Corrected Sunspot History Suggests Climate Change since the Industrial Revolution not due to Natural Solar Trends. https://www.iau.org/news/pressreleases/detail/iau1508/ (last access 23.08.2023)

Measurlabs: GC-FID. https://measurlabs.com/methods/gc-fid-analysis/ (last access 24.09.2023)